Clinical and Translational Report

Cell Host & Microbe

Development of a Human Antibody Cocktail that Deploys Multiple Functions to Confer Pan-Ebolavirus Protection

Graphical Abstract

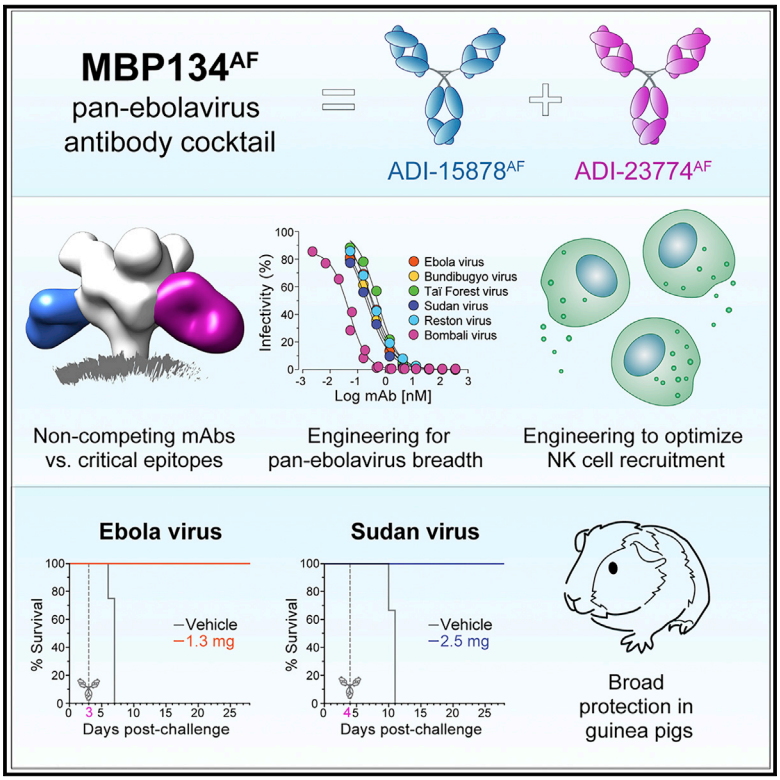

Authors

Anna Z. Wec, Zachary A. Bornholdt, Shihua He, ..., Larry Zeitlin, Xiangguo Qiu, Kartik Chandran

Correspondence

larry.zeitlin@mappbio.com (L.Z.), xiangguo.qiu@canada.ca (X.Q.), kartik.chandran@einstein.yu.edu (K.C.)

In Brief

Broadly protective therapies against filoviruses are urgently needed. Wec et al. advance a cocktail of two human mAbs as a candidate pan-ebolavirus therapeutic. The mAbs were selected for antiviral potency and breadth, engineered to enhance breadth and Fc effector functions, and tested against multiple ebolaviruses in guinea pig models of lethal challenge.

Highlights

- Cocktail of two human mAbs affording pan-ebolavirus neutralization was selected
- Cocktail outperforms single antibody in protecting against EBOV infection in guinea pigs
- Second-generation cocktail with optimized Fc effector functions enhances protection
- Single low dose of optimized cocktail protects guinea pigs against two ebolaviruses

Wec et al., 2019, Cell Host & Microbe *25*, 39–48
January 9, 2019
https://doi.org/10.1016/j.chom.2018.12.004

CellPress

Cell Host & Microbe
Clinical and Translational Report

Development of a Human Antibody Cocktail that Deploys Multiple Functions to Confer Pan-Ebolavirus Protection

Anna Z. Wec,[1,10,11] Zachary A. Bornholdt,[2,11] Shihua He,[3,11] Andrew S. Herbert,[4] Eileen Goodwin,[5] Ariel S. Wirchnianski,[1] Bronwyn M. Gunn,[6] Zirui Zhang,[3,7] Wenjun Zhu,[3,7] Guodong Liu,[3,7] Dafna M. Abelson,[2] Crystal L. Moyer,[2] Rohit K. Jangra,[1] Rebekah M. James,[4] Russell R. Bakken,[4] Natasha Bohorova,[2] Ognian Bohorov,[2] Do H. Kim,[2] Michael H. Pauly,[2] Jesus Velasco,[2] Robert H. Bortz III,[1] Kevin J. Whaley,[2] Tracey Goldstein,[8] Simon J. Anthony,[9] Galit Alter,[6] Laura M. Walker,[5] John M. Dye,[4] Larry Zeitlin,[2,13,*] Xiangguo Qiu,[3,7,13,*] and Kartik Chandran[1,12,13,14,*]

[1]Department of Microbiology and Immunology, Albert Einstein College of Medicine, Bronx, NY 10461, USA
[2]Mapp Biopharmaceutical, San Diego, CA 92121, USA
[3]Special Pathogens Program, National Microbiology Laboratory, Public Health Agency of Canada, Winnipeg, MB R3E 3R2, Canada
[4]U.S. Army Medical Research Institute of Infectious Diseases, Fort Detrick, Frederick, MD 21702, USA
[5]Adimab, LLC, Lebanon, NH 03766, USA
[6]Ragon Institute of MGH, MIT, and Harvard, Cambridge, MA 02139, USA
[7]Department of Medical Microbiology, University of Manitoba, Winnipeg, MB R3E 0J9, Canada
[8]One Health Institute and Karen C. Drayer Wildlife Health Center, School of Veterinary Medicine, University of California, Davis, Davis, CA 95616, USA
[9]Center for Infection and Immunity, Mailman School of Public Health, Columbia University, New York, NY 10032, USA
[10]Present address: Adimab, LLC, Lebanon, NH 03766, USA
[11]These authors contributed equally
[12]Twitter: @chandranlab
[13]Senior author
[14]Lead Contact
*Correspondence: larry.zeitlin@mappbio.com (L.Z.), xiangguo.qiu@canada.ca (X.Q.), kartik.chandran@einstein.yu.edu (K.C.)
https://doi.org/10.1016/j.chom.2018.12.004

SUMMARY

Passive administration of monoclonal antibodies (mAbs) is a promising therapeutic approach for Ebola virus disease (EVD). However, all mAbs and mAb cocktails that have entered clinical development are specific for a single member of the *Ebolavirus* genus, Ebola virus (EBOV), and ineffective against outbreak-causing Bundibugyo virus (BDBV) and Sudan virus (SUDV). Here, we advance MBP134, a cocktail of two broadly neutralizing human mAbs, ADI-15878 from an EVD survivor and ADI-23774 from the same survivor but specificity-matured for SUDV GP binding affinity, as a candidate pan-ebolavirus therapeutic. MBP134 potently neutralized all ebolaviruses and demonstrated greater protective efficacy than ADI-15878 alone in EBOV-challenged guinea pigs. A second-generation cocktail, MBP134^{AF}, engineered to effectively harness natural killer (NK) cells afforded additional improvement relative to its precursor in protective efficacy against EBOV and SUDV in guinea pigs. MBP134^{AF} is an optimized mAb cocktail suitable for evaluation as a pan-ebolavirus therapeutic in nonhuman primates.

INTRODUCTION

Viruses of the family *Filoviridae* (filoviruses) cause outbreaks of a lethal disease for which no FDA-approved treatments or vaccines are available. During the unprecedented 2013–2016 Ebola virus disease (EVD) epidemic in Western Africa and in its aftermath, the passive administration of monoclonal antibodies (mAbs) emerged as a promising treatment approach (Corti et al., 2016; Mire et al., 2017; Olinger et al., 2012; Pascal et al., 2018; Qiu et al., 2013, 2014, 2016). To date, three mAbs and mAb cocktails—ZMapp, REGN-EB3, and mAb114/VRC 608—have entered clinical development (National Institutes of Health Clinical Center, 2018; Davey et al., 2016; Sivapalasingam et al., 2018). However, all of these investigational treatments suffer a key liability—they are specific for a single member of the *Ebolavirus* genus, Ebola virus (EBOV), and ineffective against the divergent outbreak-causing ebolaviruses, Bundibugyo virus (BDBV) and Sudan virus (SUDV) (Corti et al., 2016; Murin et al., 2014; Pascal et al., 2018; Saphire et al., 2018), which accounted for ≈40% of all ebolavirus infections prior to 2013 (Burk et al., 2016). New broadly active immunotherapeutics are thus needed to combat the urgent public health threat posed by BDBV and SUDV, and the potential health threat posed by novel ebolaviruses yet to emerge into human populations, such as the recently described Bombali virus (BOMV) (Goldstein et al., 2018).

To discover broadly protective human antibodies, we previously isolated and characterized 349 GP-specific mAbs from a

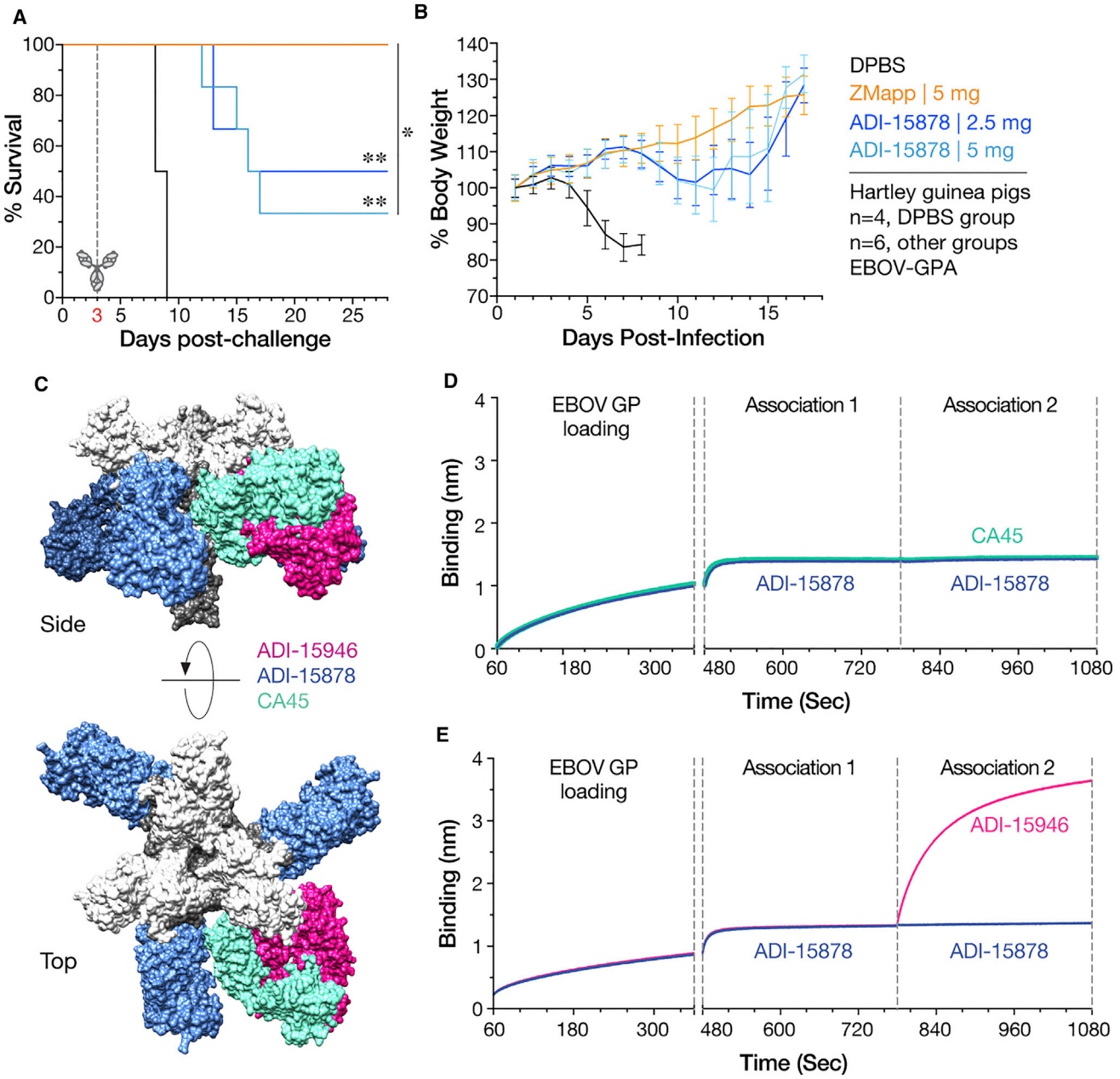

Figure 1. Selection of ADI-15946 as a Candidate Cocktail Partner for ADI-15878

(A) Hartley guinea pigs were challenged with guinea pig-adapted EBOV (EBOV-GPA) and then treated with single doses of ZMapp, ADI-15878, or vehicle (Dulbecco's phosphate-buffered saline, DPBS) at 3 days post-exposure. Survival curves (vehicle versus test mAb and ZMapp [5 mg] versus ADI-15878 [5 mg]) were compared by Mantel-Cox test. $^{**}p < 0.01$. $^{*}p < 0.05$.

(B) Body weights of surviving animals in each treatment group in (A). Averages ± SD (n = 6 for ZMapp, n = 3–6 for ADI-15878) are shown. Data are from single cohorts.

(C) *In silico* models of the ADI-15878, ADI-15946, and CA45 Fabs were fitted into negative-stain EM reconstructions of GP:Fab complexes (Wec et al., 2017; Zhao et al., 2017) and are superimposed onto a single EBOV GP structure (PDB: 5JQ337) to illustrate the approximate binding footprint and angle of approach of ADI-15946 and CA45 relative to ADI-15878. Light gray and dark gray, GP1 and GP2 subunits, respectively.

(D and E) Analysis of competitive binding of candidate IgGs to EBOV GP by biolayer interferometry (BLI). Each GP-bearing probe was sequentially dipped in analyte solutions containing ADI-15878 and then ADI-15878 (D and E, control), CA45 (D), or ADI-15946 (E). Results from a representative experiment are shown.

survivor of the West African EVD epidemic (Bornholdt et al., 2016). A systematic analysis of this library for breadth of the neutralizing mAb response against ebolaviruses identified ADI-15878 as a promising candidate therapeutic (Wec et al., 2017). ADI-15878 possesses potent pan-ebolavirus neutralizing activity through its recognition of a highly conserved conformational

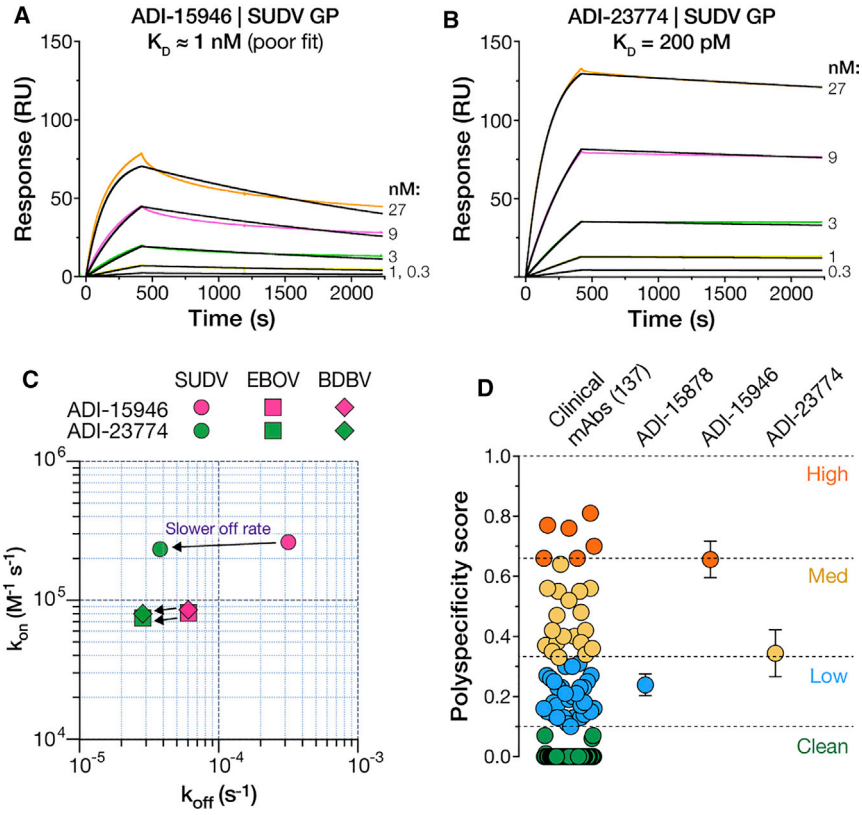

Figure 2. Binding and Polyspecificity Properties of ADI-15946 and Its Specificity-Matured Variant ADI-23774

(A and B) BLI sensorgrams for IgG-SUDV GP interactions with ADI-15946 (A) and ADI-23774 (B). Experimental curves (colored traces) were fit using a 1:1 binding model (black traces). The corresponding flow analyte (GP) concentration is indicated at the right of each curve.

(C) Comparison of association (k_{on}) and dissociation (k_{off}) rate constants for IgG interactions with EBOV, BDBV, and SUDV GP. Arrows indicate changes in the values of these constants following ADI-15946 specificity maturation.

(D) Polyspecificity scores for candidate mAbs were determined as described previously (Xu et al., 2013). The scores for 137 mAbs in commercial clinical development (Jain et al., 2017) are shown for comparison. Averages ± SD (n = 3 for ADI-15878 and ADI-15946, n = 2 for ADI-23774) from 2–3 independent experiments.

See also Figure S1 for specificity maturation of ADI-15946 to ADI-23774 and Figure S2 for GP:mAb kinetic binding constants derived from BLI.

fusion-loop epitope in GP with subnanomolar affinity and enhanced targeting of a cleaved GP intermediate generated in late endosomes. *In vivo*, ADI-15878 fully protected mice challenged with EBOV and SUDV (Bornholdt et al., 2016; Wec et al., 2017). However, monotherapy with ADI-15878 was only partially protective in ferrets (Wec et al., 2017) and guinea pigs (Figure 1A; this study), supporting prior observations that mAb cocktails targeting multiple GP epitopes may be necessary for complete protection (Flyak et al., 2016; Oswald et al., 2007; Qiu et al., 2013, 2014; Wec et al., 2017; Zhao et al., 2017).

Here, we screened existing human and nonhuman primate mAbs for a suitable partner to ADI-15878 and identified a previously described human neutralizing mAb, ADI-15946, which recognizes a broadly conserved but non-overlapping epitope in the base subdomain of ebolavirus GP (Bornholdt et al., 2016; Wec et al., 2017). Complementing data-driven mAb selection with the optimization of mAb combining sites and Fc effector functions afforded a two-mAb cocktail, $MBP134^{AF}$, which could fully protect guinea pigs against EBOV and SUDV challenge with a single ≈10 mg/kg dose administered as late as 3–5 days post-virus exposure. Our findings set the stage for evaluation of $MBP134^{AF}$ as a pan-ebolavirus therapeutic in nonhuman primates (Bornholdt et al., 2019).

RESULTS AND DISCUSSION

Identification of Candidate Partner mAbs for ADI-15878

Because previous work has demonstrated the predictive value of the guinea pig models of ebolavirus challenge for therapeutic antibody efficacy in nonhuman primates (Cross et al., 2015; Marzi, 2017; Wong et al., 2012), we exposed guinea pigs to a uniformly lethal dose of guinea pig-adapted EBOV (EBOV-GPA) (Connolly et al., 1999) and then treated them with equivalent doses of ADI-15878 or the ZMapp cocktail (Qiu et al., 2014) at 3 days post-challenge. Monotherapy with ADI-15878 afforded only 33%–50% survival and was less effective than ZMapp (100% survival) (Figures 1A and 1B), suggesting the need to target an additional GP epitope to achieve complete protection.

Potential ADI-15878 partner mAbs were filtered on the basis of (1) their host origin (human or nonhuman primate); (2) neutralization potency (50% inhibition of EBOV infectivity [IC_{50}] < 10 nM); (3) anti-ebolavirus binding and neutralization breadth (recognition and neutralization of EBOV, BDBV, and SUDV); (4) neutralization of both uncleaved and endosomally cleaved forms of ebolavirus GP, a feature previously associated with antiviral potency and breadth (Wec et al., 2017; Zhao et al., 2017); (5) lack of cross-reactivity with the secreted glycoprotein sGP present at high levels in EVD patients (to prevent sGP from "soaking up" circulating mAbs) (Mohan et al., 2012; Sanchez et al., 1996; Volchkov et al., 1995); and (6) demonstrated post-exposure protection against EBOV in mice. This selection process yielded two candidates, ADI-15946 (Bornholdt et al., 2016; Wec et al., 2017) and CA45 (Zhao et al., 2017). Like ADI-15878, these broadly neutralizing mAbs recognize conserved conformational epitopes in the "base" subdomain of the trimeric GP spike (Figure 1C), raising the possibility that they can compete with ADI-15878 for GP binding and limit cocktail efficacy. Indeed, preincubation of EBOV GP with saturating amounts of ADI-15878 abolished binding by CA45 in a biolayer interferometry (BLI) assay (Figure 1D) but did not interfere with ADI-15946 binding (Figure 1E),

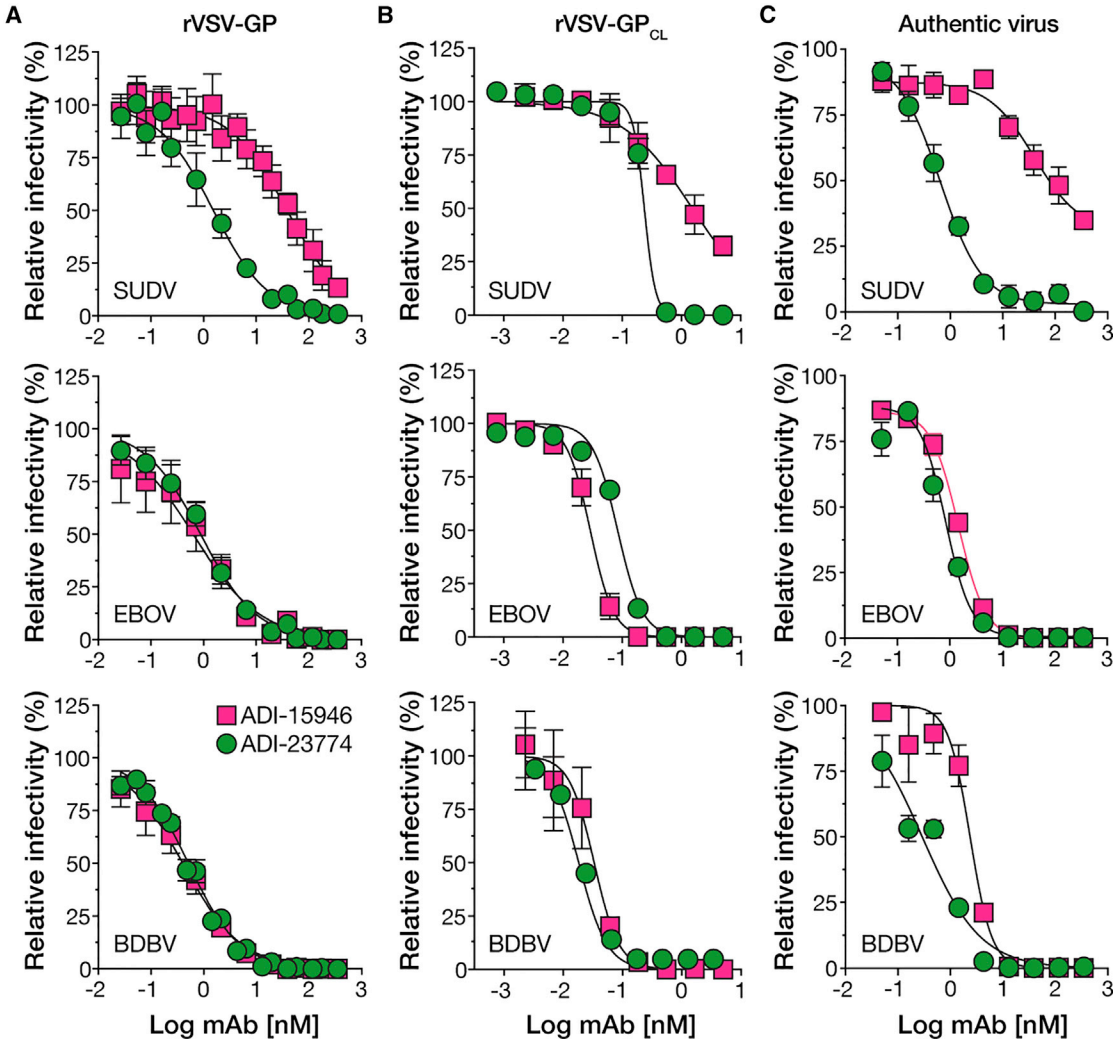

Figure 3. Neutralizing Activity of ADI-23774

(A and B) Neutralization of rVSVs encoding enhanced green fluorescent protein (eGFP) and bearing uncleaved (A) or cleaved (B) ebolavirus GP proteins (rVSV-GP and rVSV-GP$_{CL}$, respectively). Pink squares, ADI-15946. Green circles, ADI-23774. Virions were preincubated with increasing concentrations of each mAb and then exposed to cells for 12 to 14 hr at 37°C. Infection was measured by automated counting of eGFP+ cells and normalized to infection obtained in the absence of antibody. Averages ± SD (n = 6–9 in A, n = 3 in B) from 3 independent experiments.

(C) Neutralization of authentic filoviruses measured in a microneutralization assay. Virions were preincubated with increasing concentrations of each mAb and then exposed to cells for 48 hr at 37°C. Infected cells were immunostained for viral antigen and enumerated by automated fluorescence microscopy. Averages ± SD (n = 2–4) from two independent experiments.

indicating that ADI-15878 and CA45 compete for GP recognition, whereas ADI-15878 and ADI-15946 do not. Therefore, we selected ADI-15946 for further evaluation as a cocktail partner for ADI-15878.

Specificity Maturation of ADI-15946 to SUDV GP

We previously showed that ADI-15946 neutralizes EBOV, BDBV, and SUDV; however, it is less potent against SUDV (Wec et al., 2017) (Figures 3A–3C). This neutralization deficit arises from the reduced binding affinity of ADI-15946 for SUDV GP relative to EBOV GP (Figures 2A and S2A), consistent with the sequence divergence between these glycoproteins at the proposed sites of mAb contact (Wec et al., 2017). To ensure that our mAb cocktail effectively targets all known virulent ebolaviruses at two distinct sites, we sought to specificity-mature ADI-15946 to SUDV GP using yeast-display technology (Xu et al., 2013). Libraries were generated by introducing diversity into the ADI-15946 heavy and light chains (HC and LC, respectively) through oligonucleotide-based mutagenesis and transformation into *Saccharomyces cerevisiae* by homologous recombination. Improved variants were identified after 2 (LC) or 3 (HC) rounds of selection with a recombinant SUDV GP protein (Figure S1), and cross-screening for retention of EBOV and BDBV binding was performed on the best SUDV GP binder, ADI-23774 (Figures S2A–S2C). Combining beneficial LC and HC mutations yielded a variant, ADI-23774, with 5–10× enhanced binding affinity to SUDV GP and slightly improved binding to EBOV

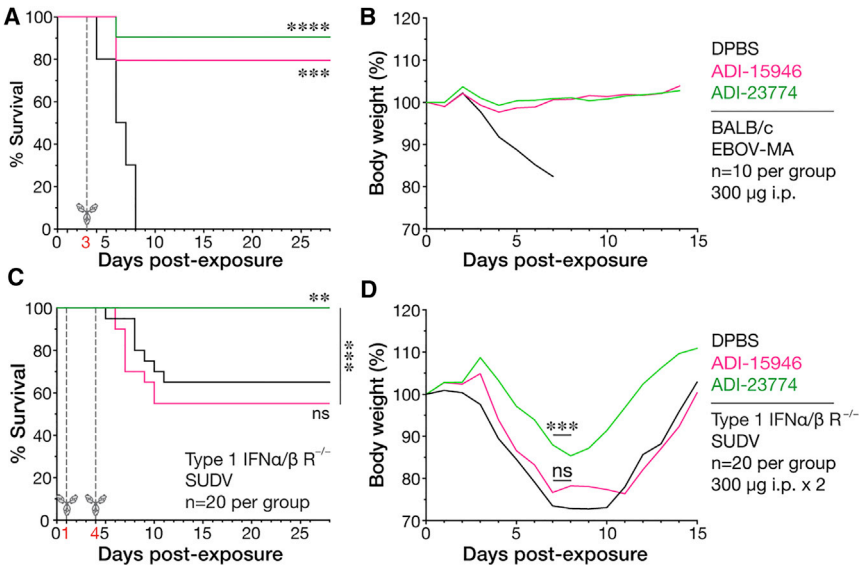

Figure 4. Protective Efficacy of ADI-23774 against Ebolavirus Challenge in Mice

(A) BALB/c mice were challenged with mouse-adapted EBOV (EBOV-MA) and then treated with single doses of the indicated mAbs or vehicle (DPBS) at 3 days post-exposure. Survival curves (vehicle versus test mAb) were compared by Mantel-Cox test.

(B) Combined body weights of surviving animals in each treatment group in (A).

Data in (A) and (B) are from single cohorts.

(C) Type 1 IFNα/β $R^{-/-}$ mice were challenged with wild-type SUDV and then treated with two doses of the indicated mAbs or vehicle (DPBS) at 1 and 4 days post-exposure. Survival curves (vehicle versus test mAb and ADI-15946 versus ADI-23774) were compared by Mantel-Cox test.

(D) Combined body weights of surviving animals in each treatment group in (C). Groups (vehicle versus test mAb) were compared by two-way ANOVA with repeated measures and Dunnett's test. Significance values for comparison of body weights on days 6–7 are shown.

Data in (C) and (D) are pooled from two cohorts. ****$p < 0.0001$. ***$p < 0.001$. **$p < 0.01$. *$p < 0.05$. ns, $p > 0.05$.

and BDBV GP relative to its ADI-15946 parent (Figures 2 and S2A–S2C). These gains in GP:mAb affinity effected by specificity maturation were primarily driven by reductions in the dissociation rate constant (k_{off}) (Figures 2C and S2D). Next, because *in vitro* affinity maturation can increase antibody polyspecificity with potential risks of off-target binding and reduced serum half-life *in vivo* (Hötzel et al., 2012), we assessed the polyspecificity of ADI-15946 and ADI-23774 as described (Jain et al., 2017; Xu et al., 2013). Fortuitously, specificity maturation also reduced ADI-23774's nonspecific binding relative to that of ADI-15946 (Figure 2D). Thus, both ADI-15878 and ADI-23774 display a low level of polyspecificity, a highly desirable property for early-stage therapeutic candidates.

Antiviral Neutralization Potency and Breadth of ADI-23774 *In Vitro*

To evaluate the breadth and potency of neutralization by ADI-23774, we performed dose-response neutralization assays with recombinant vesicular stomatitis viruses (rVSVs) bearing GPs from SUDV, EBOV, and BDBV (Figures 3A and 3B) and with authentic SUDV, EBOV, and BDBV (Figure 3C). Concordant with ADI-23774's improved binding to both recombinant GP proteins (Figures 2, S2B, and S2C) and rVSVs bearing full-length transmembrane GP (Figure S2A), ADI-23774 neutralized both rVSV-SUDV GP (Figure 3A) and authentic SUDV (Figure 3C) more potently than did ADI-15946 (IC_{50} [±95% confidence intervals] = 1 ± 1 nM for ADI-23774 versus 35 ± 1 nM for ADI-15946 against rVSV-SUDV GP; Figure 3A). Further, ADI-23774 could neutralize rVSV-SUDV GP and authentic SUDV completely without leaving an un-neutralized fraction, whereas ADI-15946 could not (Figures 3A and 3C). These trends were also apparent against rVSV-SUDV GP_{CL}, bearing a proteolytically cleaved form of GP (GP_{CL}) resembling an endosomal entry intermediate (Figure 3B). ADI-23774's increased effectiveness against SUDV did not compromise its capacity to neutralize rVSVs bearing EBOV and BDBV GP or the authentic agents (Figures 3A and 3C).

Protective Efficacy and Breadth of ADI-23774 in Mice

To assess the effects of these gains in neutralization potency on mAb protective efficacy, we evaluated ADI-23774 in murine models of EBOV (Bray et al., 1998) and SUDV (Brannan et al., 2015) challenge. ADI-23774 resembled ADI-15946 in its capacity to protect animals from challenge with mouse-adapted EBOV (EBOV-MA) when administered 3 days post-exposure (Figures 4A and 4B). However, unlike ADI-15946, which conferred no benefit against SUDV (Wec et al., 2017), ADI-23774 stemmed weight loss in SUDV-challenged interferon α/β receptor-knockout (IFNα/β $R^{-/-}$) mice and fully protected them when administered 1 and 4 days post-exposure (Figures 4C and 4D). Thus, ADI-23774 is an optimized candidate to serve as a partner mAb for ADI-15878, with enhancements over its precursor in biophysical properties, neutralization breadth, and anti-ebolavirus protective breadth in mice.

In Vitro Neutralization Properties of a Cocktail Comprising ADI-15878 and ADI-23774 and Its Protective Efficacy in Guinea Pigs

We combined ADI-15878 and ADI-23774 into a cocktail, MBP134, and examined its functional properties *in vitro*. MBP134 potently neutralized rVSVs bearing GP proteins from ebolaviruses belonging to all six species, including BOMV, recently discovered in free-tailed bats in Sierra Leone (Figure 5). Cultivation of rVSV-EBOV GP in the presence of MBP134 yielded a single escape mutant genotype after seven serial passages; however, this mutant was only partially resistant to MBP134 neutralization (data not shown). MBP134's capacity to broadly and effectively neutralize ebolaviruses suggests that its utility

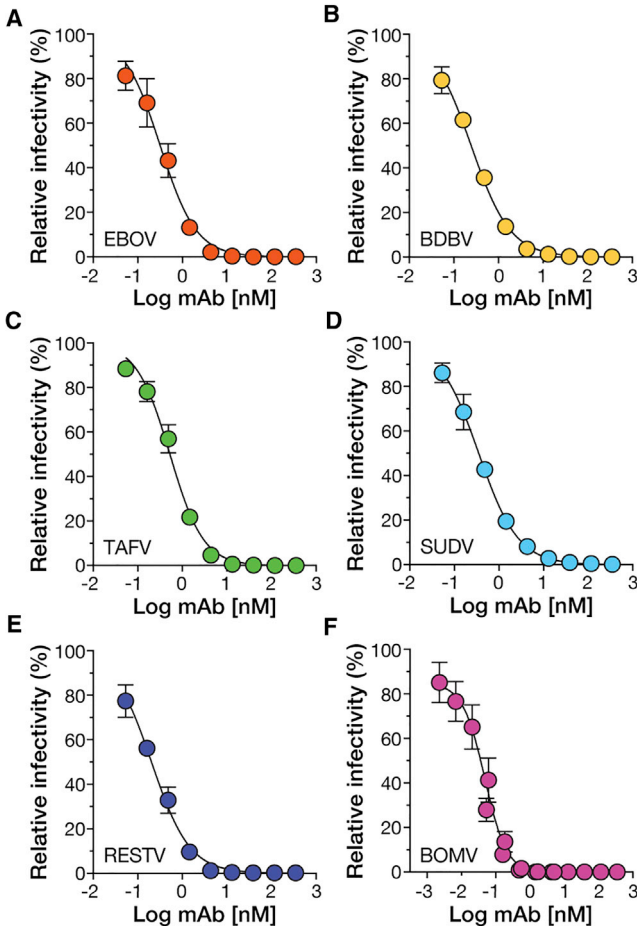

Figure 5. Neutralizing Activity of MBP134 Cocktail

Neutralization of rVSVs encoding eGFP and bearing GP proteins from EBOV (A), BDBV (B), Taï Forest virus (TAFV) (C), SUDV (D), Reston virus (RESTV) (E), and BOMV (F) was determined as in Figure 3. Averages ± SD (n = 6) from three independent experiments are shown.

could extend beyond the currently recognized agents to unknown viruses and viral variants that may pose a spillover risk in the future.

To evaluate the protective potential of MBP134, we exposed guinea pigs to a uniformly lethal dose of EBOV-GPA and then treated them with increasing doses of MBP134 at 3 days post-challenge (Figures 6A and 6B). Treatment with 2.5–3.3 mg MBP134 (total mAb dose) per animal afforded near complete protection (Figure 6A), whereas treatment with ADI-15878 alone at 2.5–5 mg per animal afforded ≤50% protection (Figure 1A), providing evidence for the superior efficacy of the cocktail over the monotherapy (see Table S1 for statistical comparisons of survival curves in Figure 6A).

Optimization of MBP134-Mediated Immune Effector Functions *In Vitro* through Fc Glycan Engineering

To further enhance the *in vivo* potency of MBP134, we set out to optimize an orthogonal property of its component mAbs—their capacity to harness the host antiviral innate immune response through antigen-dependent engagement of activating Fc receptors on immune cells. Because cytolysis by NK cells has been demonstrated to play a critical role in protection against EBOV infection (Gunn et al., 2018; Warfield et al., 2004), we measured the EBOV GP-dependent activation of human NK cells derived from four seronegative human donors by ADI-15878 and ADI-23774. Both mAbs were poorly active, as judged by their limited capacity to induce three markers of NK cell activation—degranulation (Figure 7A), and production of IFN-γ (Figure 7B) and MIP-1β (Figure 7C)—relative to the ZMapp component mAb c13C6 (Qiu et al., 2014) (also see Figure S3). Thus, viral neutralization is likely the primary mode of MBP134's antiviral activity. We postulated that NK cell recruitment, activation, and infected-cell killing by MBP134 could be improved by enhancing its capacity to engage the activating Fc receptor FcγRIIIa on NK cells. Indeed, previous work has demonstrated that mAbs bearing uniformly afucosylated glycan structures display precisely this property (Ferrara et al., 2011; Shields et al., 2002), which has been linked to their enhanced protective efficacy against several viral pathogens, including EBOV (Forthal et al., 2010; Gunn et al., 2018; Hiatt et al., 2014; Saphire et al., 2018; Zeitlin et al., 2011). Accordingly, we generated and evaluated afucosylated variants of the MBP134 mAbs (ADI-15878^{AF} and ADI-23774^{AF}, respectively). Both variant mAbs significantly

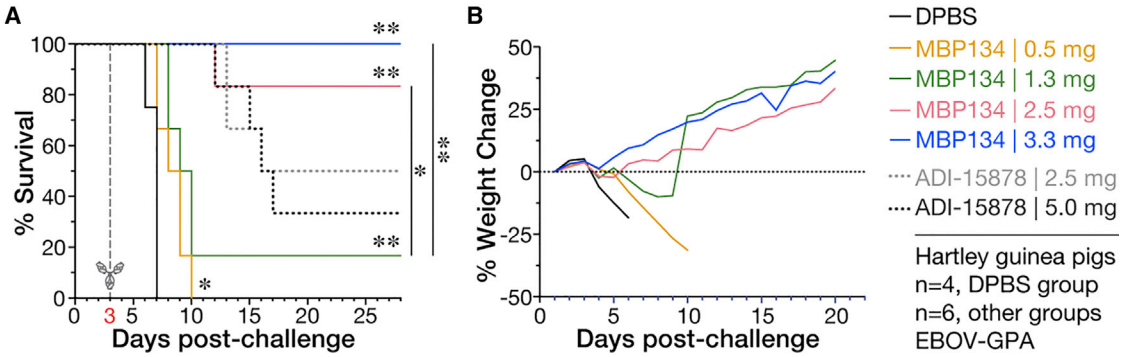

Figure 6. Protective Efficacy of MBP134 in Guinea Pigs

(A) Hartley guinea pigs were challenged with EBOV-GPA and then treated with single doses of ADI-15878, MBP134 (1:1 mixture of ADI-15878 and ADI-23774), or vehicle (DPBS) at 3 days post-exposure. Survival curves were compared by Mantel-Cox test.

(B) Body weights of surviving animals in each treatment group in (A).

Data are from single cohorts. **p < 0.01. *p < 0.05. ns, p > 0.05. See also Table S1 for statistical details on the groups compared in (A).

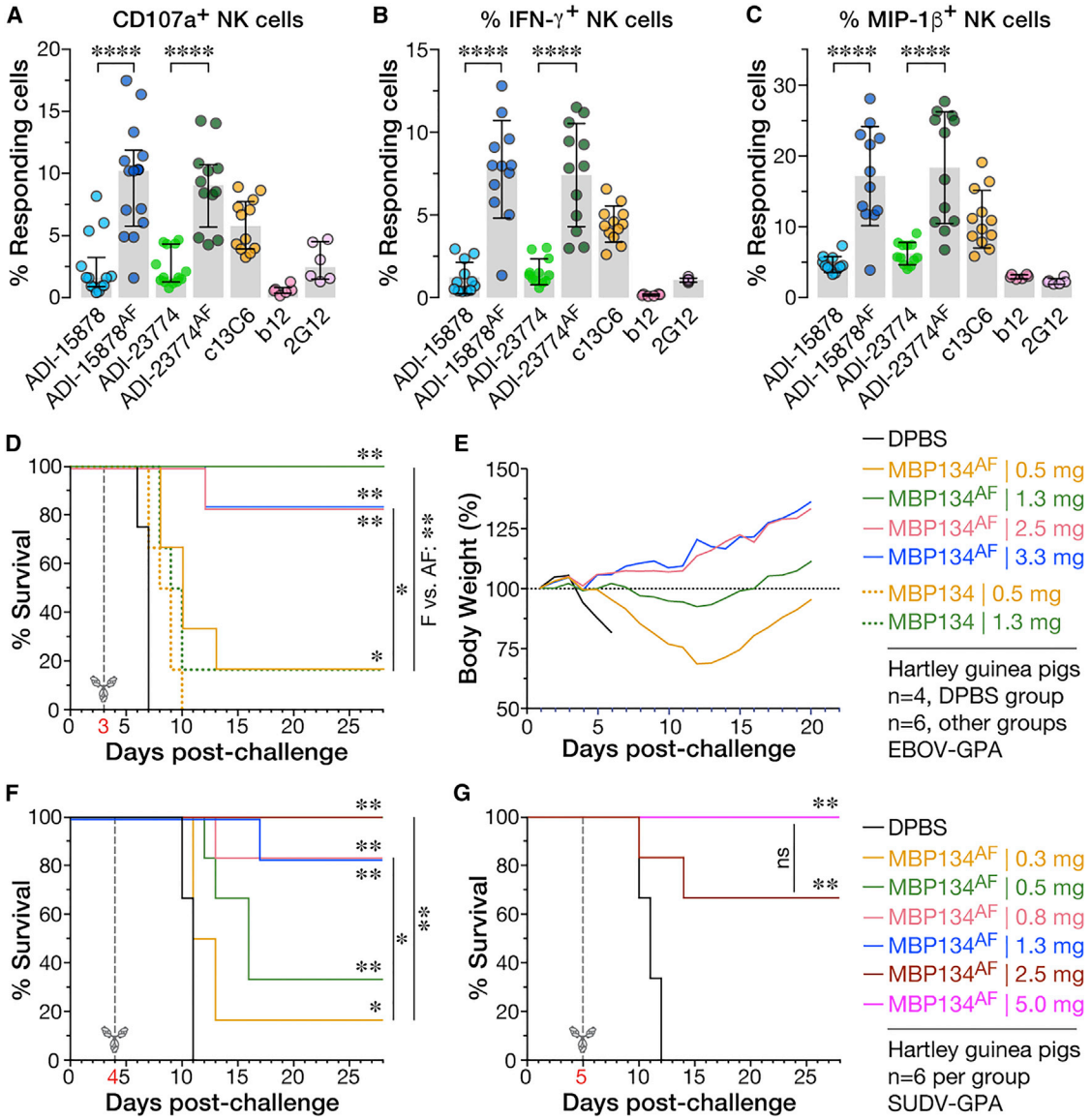

Figure 7. Development and Evaluation of the Second-Generation MBP134^{AF} Cocktail

(A–C) Activation of human natural killer (NK) cells by EBOV GP:IgG complexes. NK cells enriched from the peripheral blood of four different human donors were incubated with complexes between EBOV GP and the indicated IgGs (10 μg/mL) for 5 hr at 37°C, and then stained with antibody-fluorophore conjugates specific for the cell-surface markers CD3, CD56, and CD16, followed by intracellular staining for markers of NK cell activation, CD107a (degranulation) (A), IFN-γ (B), and MIP-1β (C). CD3$^-$/CD56^{dim}/CD16$^+$ NK cells were analyzed by flow cytometry. Data with cells from all four donors are pooled. HIV-1 glycoprotein-specific mAbs b12 and 2G12 are included as (negative) controls for antigen specificity. EBOV GP-specific mAb c13C6 produced in transgenic *Nicotiana benthamiana* tobacco plants to bear a highly functional afucosylated/agalactosylated bisected glycan is included as a positive control. Averages ± SD (n = 12–14 for all mAbs except b12 and 2G12 [n = 6] from 4 independent experiments). The indicated groups were compared by one-way ANOVA and Tukey's test.

(D) Hartley guinea pigs were challenged with EBOV-GPA and then treated with single doses of MBP134, MBP134^{AF} (1:1 mixture of ADI-15878^{AF} and ADI-23774^{AF}), or vehicle (DPBS) at 3 days post-exposure.

(E) Body weights of surviving animals in each treatment group in (F).

Data in (D) and (E) are from single cohorts.

(F and G) Guinea pigs were challenged with SUDV-GPA and then treated with single doses of MBP134^{AF} or vehicle (DPBS) at 4 (F) or 5 (G) days post-exposure. Data are from single cohorts.

Survival curves in (D) and (F) were compared by Mantel-Cox test. ****$p < 0.0001$. **$p < 0.01$. *$p < 0.05$. ns, $p > 0.05$. See also Figure S3 for flow cytometric gating strategies in (A)–(C) and Table S2 for statistical details on the groups compared in (D) and (F).

outperformed their fucosylated precursors in all three NK cell activation assays (Figures 7A–7C), confirming their enhanced capacity to engage the innate immune system.

Protective Efficacy and Breadth of the MBP134^{AF} Cocktail in Guinea Pigs

Finally, we assessed the protective potential of the second-generation MBP134^{AF} cocktail in guinea pigs, which possess an Fc receptor (gpFcγRIV) homologous to human FcγRIIIA with enhanced binding affinity for afucosylated human IgGs relative to their fucosylated counterparts (Mao et al., 2017). Only 1.3 mg (total mAb dose) MBP134^{AF} administered at 3 days post-challenge was required to fully protect animals from EBOV-GPA (Figures 7D and 7E)—an approximately 2-fold reduction in dosage relative to the parent MBP134 cocktail ($p = 0.0064$, 1.3 mg MBP134 versus 1.3 mg MBP134^{AF}) (Table S2). Moreover, a single MBP134^{AF} dose as low as 0.8 mg administered at 4 days post-challenge was sufficient to protect >80% of guinea pigs challenged with guinea pig-adapted SUDV (SUDV-GPA) (Wong et al., 2015) (Figure 7F). Remarkably, MBP134^{AF} afforded 70%–100% protection from SUDV-GPA challenge (at 2.5–5.0 mg total mAb dose) even when treatment was delayed to 5 days post-challenge (Figure 7G) (see Table S2 for statistical comparisons of survival curves in Figures 7D and 7F). These are, to our knowledge, the lowest single doses (0.8–1.3 mg total mAb) and longest post-exposure treatment windows (4–5 days) demonstrated to protect guinea pigs from lethal ebolavirus challenge. All previous studies with both therapeutic mAbs and mAb cocktails used total doses of 5–10 mg and did not report initial mAb treatments past 3 days post-exposure (Flyak et al., 2016, 2018; Gilchuk et al., 2018; Howell et al., 2016; Qiu et al., 2012; Zhao et al., 2017).

Summary and Concluding Remarks

Herein, we have used a rigorous mAb selection strategy coupled to yeast-based specificity maturation and Fc glycan engineering to develop a next-generation human mAb cocktail, MBP134^{AF}, which can protect against EBOV and SUDV in small and large rodents. MBP134^{AF} targets all known ebolavirus GP proteins (including that from a recently discovered "pre-emergent" agent; Goldstein et al., 2018); recognizes GPs from EBOV, BDBV, TAFV, SUDV, and BOMV at two independent antigenic sites; and neutralizes both the extracellular and endosomal intermediate forms of GP, thereby conferring potency as well as robustness to viral neutralization escape. Further, it is optimized to leverage both mechanical neutralization and Fc-linked innate immune functions to block viral infection and spread. By virtue of these advanced features, MBP134^{AF} affords unparalleled improvements in therapeutic potency against broad ebolavirus challenge in the stringent guinea pig challenge model relative to any mAbs or mAb cocktails that have been described previously. Our findings set the stage for evaluation of MBP134^{AF} as a pan-ebolavirus therapeutic in nonhuman primates (Bornholdt et al., 2019).

STAR★METHODS

Detailed methods are provided in the online version of this paper and include the following:

- KEY RESOURCES TABLE
- CONTACT FOR REAGENT AND RESOURCE SHARING
- EXPERIMENTAL MODEL AND SUBJECT DETAILS
  - Cell Lines
  - Culture of Primary Human Innate Immune Cells
  - Ethics Statement for Primary Human Innate Immune Cells
  - Mice
  - Guinea Pigs
  - Animal Welfare Statement
  - Recombinant Vesicular Stomatitis Viruses (rVSVs)
  - Authentic Filoviruses
- METHOD DETAILS
  - Expression and Purification of mAbs
  - Expression and Purification of Recombinant GP Ectodomains
  - VSV Infectivity Measurements and Neutralization Assays
  - Authentic Filovirus Microneutralization Assays
  - ADI-15946 Affinity Maturation
  - GP:mAb Binding ELISA
  - GP:mAb Kinetic Binding Analysis by Biolayer Interferometry (BLI)
  - GP:mAb Kinetic Binding Analysis by Surface Plasmon Resonance (SPR)
  - Antibody-Mediated Activation of Human NK (Natural Killer) Cells
  - EBOV and SUDV Challenge Studies in Mice
  - EBOV and SUDV Challenge Studies in Guinea Pigs
- QUANTIFICATION AND STATISTICAL ANALYSIS
  - Statistical Analysis

SUPPLEMENTAL INFORMATION

Supplemental Information includes three figures and two tables and can be found with this article online at https://doi.org/10.1016/j.chom.2018.12.004.

ACKNOWLEDGMENTS

We thank T. Krause, C. Harold, T. Alkutkar, and I. Gutierrez for technical support and laboratory management. We thank M.J. Aman for provision of mAb CA45. This work is supported by NIH grants AI134824 and AI132256 (to K.C.) and U19AI109762 (to KC., J.M.D., and L.Z.), and by the Public Health Agency of Canada (to X.Q.). L.Z., X.Q., D.M.A., and Z.A.B. were additionally supported by DTRA contract HDTRA1-13-C-0018. K.C. was additionally supported by an Irma T. Hirschl/Monique Weill-Caulier Research Award. Opinions, conclusions, interpretations, and recommendations are those of the authors and are not necessarily endorsed by the U.S. Army. The mention of trade names or commercial products does not constitute endorsement or recommendation for use by the Department of the Army or the Department of Defense.

AUTHOR CONTRIBUTIONS

Conceptualization, A.Z.W., Z.A.B., A.S.H., L.M.W., J.M.D., L.Z., X.Q., and K.C.; Methodology, A.Z.W., A.S.H., G.A., L.M.W., J.M.D., X.Q., and K.C.; Investigation, A.Z.W., Z.A.B., S.H., A.S.H., E.G., A.S.W., B.M.G., Z.Z., W.Z., G.L., D.M.A., C.L.M., R.K.J., R.M.J., R.R.B., N.B., O.B., D.H.K., M.H.P., J.V., and R.H.B.; Writing – Original Draft, A.Z.W. and K.C.; Writing – Review & Editing, A.Z.W., Z.A.B., A.S.H., A.S.W., B.M.G., R.K.J., T.G., S.J.A., L.M.W., J.M.D., L.Z., X.Q., and K.C.; Visualization, A.Z.W., Z.A.B., A.S.H., and K.C.; Funding Acquisition, J.M.D., L.Z., X.Q., and K.C.; Resources, T.G. and S.J.A.; Supervision, Z.A.B., A.S.H., K.J.W., G.A., L.M.W., J.M.D., L.Z., X.Q., and K.C.

DECLARATION OF INTERESTS

A.Z.W., Z.A.B., L.Z., L.M.W., and K.C. are co-inventors on a provisional patent application (No. 62/460,200) assigned to Mapp Biopharmaceutical, Inc., Adimab LLC, and Albert Einstein College of Medicine, Inc. describing the development and use of MBP134 and variants thereof for anti-ebolavirus immunotherapy. A.Z.W., E.G., and L.M.W. are employees and shareholders in Adimab LLC. Z.A.B., D.M.A., C.L.M., N.B., O.B., D.H.K., M.H.P., J.V., K.J., and L.Z. are employees and shareholders in Mapp Biopharmaceutical, Inc. K.J. and L.Z. are CEO and President of Mapp Biopharmaceutical, Inc., respectively. K.C. and J.M.D. are Scientific Advisory Board members of Integrum Scientific, LLC.

Received: September 20, 2018
Revised: October 28, 2018
Accepted: November 21, 2018
Published: January 9, 2019

REFERENCES

Bornholdt, Z.A., Turner, H.L., Murin, C.D., Li, W., Sok, D., Souders, C.A., Piper, A.E., Goff, A., Shamblin, J.D., Wollen, S.E., et al. (2016). Isolation of potent neutralizing antibodies from a survivor of the 2014 Ebola virus outbreak. Science *351*, 1078–1083.

Bornholdt, Z.A., Herbert, A.S., Mire, C.E., He, S., Cross, R.W., Wec, A.Z., Abelson, D.M., Geisbert, J.B., James, R.M., Rahim, M.N., et al. (2019). A two-antibody pan-ebolavirus cocktail confers broad therapeutic protection in ferrets and nonhuman primates. Cell Host Microbe *25*, this issue, 49–58.

Brannan, J.M., Froude, J.W., Prugar, L.I., Bakken, R.R., Zak, S.E., Daye, S.P., Wilhelmsen, C.E., and Dye, J.M. (2015). Interferon α/β receptor-deficient mice as a model for Ebola virus disease. J. Infect. Dis. *212* (*Suppl 2*), S282–S294.

Bray, M., Davis, K., Geisbert, T., Schmaljohn, C., and Huggins, J. (1998). A mouse model for evaluation of prophylaxis and therapy of Ebola hemorrhagic fever. J. Infect. Dis. *178*, 651–661.

Burk, R., Bollinger, L., Johnson, J.C., Wada, J., Radoshitzky, S.R., Palacios, G., Bavari, S., Jahrling, P.B., and Kuhn, J.H. (2016). Neglected filoviruses. FEMS Microbiol. Rev. *40*, 494–519.

Chao, G., Lau, W.L., Hackel, B.J., Sazinsky, S.L., Lippow, S.M., and Wittrup, K.D. (2006). Isolating and engineering human antibodies using yeast surface display. Nat. Protoc. *1*, 755–768.

Connolly, B.M., Steele, K.E., Davis, K.J., Geisbert, T.W., Kell, W.M., Jaax, N.K., and Jahrling, P.B. (1999). Pathogenesis of experimental Ebola virus infection in guinea pigs. J. Infect. Dis. *179* (*Suppl 1*), S203–S217.

Corti, D., Misasi, J., Mulangu, S., Stanley, D.A., Kanekiyo, M., Wollen, S., Ploquin, A., Doria-Rose, N.A., Staupe, R.P., Bailey, M., et al. (2016). Protective monotherapy against lethal Ebola virus infection by a potently neutralizing antibody. Science *351*, 1339–1342.

Cross, R.W., Fenton, K.A., Geisbert, J.B., Mire, C.E., and Geisbert, T.W. (2015). Modeling the disease course of Zaire ebolavirus infection in the outbred guinea pig. J. Infect. Dis. *212* (*Suppl 2*), S305–S315.

Davey, R.T., Jr., Dodd, L., Proschan, M.A., Neaton, J., Neuhaus Nordwall, J., Koopmeiners, J.S., Beigel, J., Tierney, J., Lane, H.C., Fauci, A.S., et al.; PREVAIL II Writing Group; Multi-National PREVAIL II Study Team (2016). A randomized, controlled trial of zmapp for ebola virus infection. N. Engl. J. Med. *375*, 1448–1456.

Ferrara, C., Grau, S., Jäger, C., Sondermann, P., Brünker, P., Waldhauer, I., Hennig, M., Ruf, A., Rufer, A.C., Stihle, M., et al. (2011). Unique carbohydrate-carbohydrate interactions are required for high affinity binding between FcgammaRIII and antibodies lacking core fucose. Proc. Natl. Acad. Sci. U S A *108*, 12669–12674.

Flyak, A.I., Shen, X., Murin, C.D., Turner, H.L., David, J.A., Fusco, M.L., Lampley, R., Kose, N., Ilinykh, P.A., Kuzmina, N., et al. (2016). Cross-reactive and potent neutralizing antibody responses in human survivors of natural ebolavirus infection. Cell *164*, 392–405.

Flyak, A.I., Kuzmina, N., Murin, C.D., Bryan, C., Davidson, E., Gilchuk, P., Gulka, C.P., Ilinykh, P.A., Shen, X., Huang, K., et al. (2018). Broadly neutralizing antibodies from human survivors target a conserved site in the Ebola virus glycoprotein HR2-MPER region. Nat. Microbiol. *3*, 670–677.

Forthal, D.N., Gach, J.S., Landucci, G., Jez, J., Strasser, R., Kunert, R., and Steinkellner, H. (2010). Fc-glycosylation influences Fcγ receptor binding and cell-mediated anti-HIV activity of monoclonal antibody 2G12. J. Immunol. *185*, 6876–6882.

Gilchuk, P., Kuzmina, N., Ilinykh, P.A., Huang, K., Gunn, B.M., Bryan, A., Davidson, E., Doranz, B.J., Turner, H.L., Fusco, M.L., et al. (2018). Multifunctional pan-ebolavirus antibody recognizes a site of broad vulnerability on the ebolavirus glycoprotein. Immunity *49*, 363–374.e10.

Goldstein, T., Anthony, S.J., Gbakima, A., Bird, B.H., Bangura, J., Tremeau-Bravard, A., Belaganahalli, M.N., Wells, H.L., Dhanota, J.K., Liang, E., et al. (2018). The discovery of Bombali virus adds further support for bats as hosts of ebolaviruses. Nat. Microbiol. *3*, 1084–1089.

Gunn, B.M., Yu, W.-H., Karim, M.M., Brannan, J.M., Herbert, A.S., Wec, A.Z., Halfmann, P.J., Fusco, M.L., Schendel, S.L., Gangavarapu, K., et al. (2018). A role for Fc function in therapeutic monoclonal antibody-mediated protection against Ebola virus. Cell Host Microbe *24*, 221–233.e5.

Hiatt, A., Bohorova, N., Bohorov, O., Goodman, C., Kim, D., Pauly, M.H., Velasco, J., Whaley, K.J., Piedra, P.A., Gilbert, B.E., and Zeitlin, L. (2014). Glycan variants of a respiratory syncytial virus antibody with enhanced effector function and in vivo efficacy. Proc. Natl. Acad. Sci. U S A *111*, 5992–5997.

Hötzel, I., Theil, F.-P., Bernstein, L.J., Prabhu, S., Deng, R., Quintana, L., Lutman, J., Sibia, R., Chan, P., Bumbaca, D., et al. (2012). A strategy for risk mitigation of antibodies with fast clearance. MAbs *4*, 753–760.

Howell, K.A., Qiu, X., Brannan, J.M., Bryan, C., Davidson, E., Holtsberg, F.W., Wec, A.Z., Shulenin, S., Biggins, J.E., Douglas, R., et al. (2016). Antibody treatment of Ebola and Sudan virus infection via a uniquely exposed epitope within the glycoprotein receptor-binding site. Cell Rep. *15*, 1514–1526.

Jahrling, P.B., Geisbert, T.W., Geisbert, J.B., Swearengen, J.R., Bray, M., Jaax, N.K., Huggins, J.W., LeDuc, J.W., and Peters, C.J. (1999). Evaluation of immune globulin and recombinant interferon-alpha2b for treatment of experimental Ebola virus infections. J. Infect. Dis. *179* (*Suppl 1*), S224–S234.

Jain, T., Sun, T., Durand, S., Hall, A., Houston, N.R., Nett, J.H., Sharkey, B., Bobrowicz, B., Caffry, I., Yu, Y., et al. (2017). Biophysical properties of the clinical-stage antibody landscape. Proc. Natl. Acad. Sci. U S A *114*, 944–949.

Mao, C., Near, R., and Gao, W. (2017). Identification of a guinea pig Fcγ receptor that exhibits enhanced binding to afucosylated human and mouse IgG. J. Infect. Dis. Med. *1*, 102.

Marzi, A. (2017). Evaluation of ebola virus countermeasures in guinea pigs. Methods Mol. Biol. *1628*, 283–291.

Mire, C.E., Geisbert, J.B., Borisevich, V., Fenton, K.A., Agans, K.N., Flyak, A.I., Deer, D.J., Steinkellner, H., Bohorov, O., Bohorova, N., et al. (2017). Therapeutic treatment of Marburg and Ravn virus infection in nonhuman primates with a human monoclonal antibody. Sci. Transl. Med. *9*, https://doi.org/10.1126/scitranslmed.aai8711.

Mohan, G.S., Li, W., Ye, L., Compans, R.W., and Yang, C. (2012). Antigenic subversion: a novel mechanism of host immune evasion by Ebola virus. PLoS Pathog. *8*, e1003065.

Murin, C.D., Fusco, M.L., Bornholdt, Z.A., Qiu, X., Olinger, G.G., Zeitlin, L., Kobinger, G.P., Ward, A.B., and Saphire, E.O. (2014). Structures of protective antibodies reveal sites of vulnerability on Ebola virus. Proc. Natl. Acad. Sci. U S A *111*, 17182–17187.

National Institutes of Health Clinical Center (2018). Safety and Pharmacokinetics of a Human Monoclonal Antibody, VRC-EBOMAB092-00-AB (MAb114) (Administered Intravenously to Healthy Adults).

Ng, M., Ndungo, E., Jangra, R.K., Cai, Y., Postnikova, E., Radoshitzky, S.R., Dye, J.M., Ramírez de Arellano, E., Negredo, A., Palacios, G., et al. (2014). Cell entry by a novel European filovirus requires host endosomal cysteine proteases and Niemann-Pick C1. Virology *468-470*, 637–646.

Olinger, G.G., Jr., Pettitt, J., Kim, D., Working, C., Bohorov, O., Bratcher, B., Hiatt, E., Hume, S.D., Johnson, A.K., Morton, J., et al. (2012). Delayed treatment of Ebola virus infection with plant-derived monoclonal antibodies

provides protection in rhesus macaques. Proc. Natl. Acad. Sci. U S A *109*, 18030–18035.

Oswald, W.B., Geisbert, T.W., Davis, K.J., Geisbert, J.B., Sullivan, N.J., Jahrling, P.B., Parren, P.W.H.I., and Burton, D.R. (2007). Neutralizing antibody fails to impact the course of Ebola virus infection in monkeys. PLoS Pathog. *3*, e9.

Pascal, K.E., Dudgeon, D., Trefry, J.C., Anantpadma, M., Sakurai, Y., Murin, C.D., Turner, H.L., Fairhurst, J., Torres, M., Rafique, A., et al. (2018). Development of clinical-stage human monoclonal antibodies that treat advanced Ebola virus disease in non-human primates. J. Infect. Dis. *218* (suppl 5), S612–S626.

Qiu, X., Fernando, L., Melito, P.L., Audet, J., Feldmann, H., Kobinger, G., Alimonti, J.B., and Jones, S.M. (2012). Ebola GP-specific monoclonal antibodies protect mice and guinea pigs from lethal Ebola virus infection. PLoS Negl. Trop. Dis. *6*, e1575.

Qiu, X., Audet, J., Wong, G., Fernando, L., Bello, A., Pillet, S., Alimonti, J.B., and Kobinger, G.P. (2013). Sustained protection against Ebola virus infection following treatment of infected nonhuman primates with ZMAb. Sci. Rep. *3*, 3365.

Qiu, X., Wong, G., Audet, J., Bello, A., Fernando, L., Alimonti, J.B., Fausther-Bovendo, H., Wei, H., Aviles, J., Hiatt, E., et al. (2014). Reversion of advanced Ebola virus disease in nonhuman primates with ZMapp. Nature *514*, 47–53.

Qiu, X., Audet, J., Lv, M., He, S., Wong, G., Wei, H., Luo, L., Fernando, L., Kroeker, A., Fausther Bovendo, H., et al. (2016). Two-mAb cocktail protects macaques against the Makona variant of Ebola virus. Sci. Transl. Med. *8*, 329ra33.

Sanchez, A., Trappier, S.G., Mahy, B.W., Peters, C.J., and Nichol, S.T. (1996). The virion glycoproteins of Ebola viruses are encoded in two reading frames and are expressed through transcriptional editing. Proc. Natl. Acad. Sci. U S A *93*, 3602–3607.

Saphire, E.O., Schendel, S.L., Fusco, M.L., Gangavarapu, K., Gunn, B.M., Wec, A.Z., Halfmann, P.J., Brannan, J.M., Herbert, A.S., Qiu, X., et al.; Viral Hemorrhagic Fever Immunotherapeutic Consortium (2018). Systematic analysis of monoclonal antibodies against Ebola virus GP defines features that contribute to protection. Cell *174*, 938–952.e13.

Shields, R.L., Lai, J., Keck, R., O'Connell, L.Y., Hong, K., Meng, Y.G., Weikert, S.H.A., and Presta, L.G. (2002). Lack of fucose on human IgG1 N-linked oligosaccharide improves binding to human Fcgamma RIII and antibody-dependent cellular toxicity. J. Biol. Chem. *277*, 26733–26740.

Sivapalasingam, S., Kamal, M., Slim, R., Hosain, R., Shao, W., Stoltz, R., Yen, J., Pologe, L.G., Cao, Y., Partridge, M., et al. (2018). Safety, pharmacokinetics, and immunogenicity of a co-formulated cocktail of three human monoclonal antibodies targeting Ebola virus glycoprotein in healthy adults: a randomised, first-in-human phase 1 study. Lancet Infect. Dis. *18*, 884–893.

Stemmer, W.P. (1994). DNA shuffling by random fragmentation and reassembly: in vitro recombination for molecular evolution. Proc. Natl. Acad. Sci. U S A *91*, 10747–10751.

Towner, J.S., Sealy, T.K., Khristova, M.L., Albariño, C.G., Conlan, S., Reeder, S.A., Quan, P.-L., Lipkin, W.I., Downing, R., Tappero, J.W., et al. (2008). Newly discovered ebola virus associated with hemorrhagic fever outbreak in Uganda. PLoS Pathog. *4*, e1000212.

Volchkov, V.E., Becker, S., Volchkova, V.A., Ternovoj, V.A., Kotov, A.N., Netesov, S.V., and Klenk, H.D. (1995). GP mRNA of Ebola virus is edited by the Ebola virus polymerase and by T7 and vaccinia virus polymerases. Virology *214*, 421–430.

Warfield, K.L., Perkins, J.G., Swenson, D.L., Deal, E.M., Bosio, C.M., Aman, M.J., Yokoyama, W.M., Young, H.A., and Bavari, S. (2004). Role of natural killer cells in innate protection against lethal ebola virus infection. J. Exp. Med. *200*, 169–179.

Wec, A.Z., Nyakatura, E.K., Herbert, A.S., Howell, K.A., Holtsberg, F.W., Bakken, R.R., Mittler, E., Christin, J.R., Shulenin, S., Jangra, R.K., et al. (2016). A "Trojan horse" bispecific-antibody strategy for broad protection against ebolaviruses. Science *354*, 350–354.

Wec, A.Z., Herbert, A.S., Murin, C.D., Nyakatura, E.K., Abelson, D.M., Fels, J.M., He, S., James, R.M., de La Vega, M.-A., Zhu, W., et al. (2017). Antibodies from a human survivor define sites of vulnerability for broad protection against ebolaviruses. Cell *169*, 878–890.e15.

Whelan, S.P., Ball, L.A., Barr, J.N., and Wertz, G.T. (1995). Efficient recovery of infectious vesicular stomatitis virus entirely from cDNA clones. Proc. Natl. Acad. Sci. U S A *92*, 8388–8392.

Wong, A.C., Sandesara, R.G., Mulherkar, N., Whelan, S.P., and Chandran, K. (2010). A forward genetic strategy reveals destabilizing mutations in the Ebolavirus glycoprotein that alter its protease dependence during cell entry. J. Virol. *84*, 163–175.

Wong, G., Richardson, J.S., Pillet, S., Patel, A., Qiu, X., Alimonti, J., Hogan, J., Zhang, Y., Takada, A., Feldmann, H., and Kobinger, G.P. (2012). Immune parameters correlate with protection against ebola virus infection in rodents and nonhuman primates. Sci. Transl. Med. *4*, 158ra146.

Wong, G., He, S., Wei, H., Kroeker, A., Audet, J., Leung, A., Cutts, T., Graham, J., Kobasa, D., Embury-Hyatt, C., et al. (2015). Development and characterization of a guinea pig-adapted Sudan virus. J. Virol. *90*, 392–399.

Xu, Y., Roach, W., Sun, T., Jain, T., Prinz, B., Yu, T.-Y., Torrey, J., Thomas, J., Bobrowicz, P., Vásquez, M., et al. (2013). Addressing polyspecificity of antibodies selected from an in vitro yeast presentation system: a FACS-based, high-throughput selection and analytical tool. Protein Eng. Des. Sel. *26*, 663–670.

Zeitlin, L., Pettitt, J., Scully, C., Bohorova, N., Kim, D., Pauly, M., Hiatt, A., Ngo, L., Steinkellner, H., Whaley, K.J., and Olinger, G.G. (2011). Enhanced potency of a fucose-free monoclonal antibody being developed as an Ebola virus immunoprotectant. Proc. Natl. Acad. Sci. U S A *108*, 20690–20694.

Zhao, X., Howell, K.A., He, S., Brannan, J.M., Wec, A.Z., Davidson, E., Turner, H.L., Chiang, C.-I., Lei, L., Fels, J.M., et al. (2017). Immunization-elicited broadly protective antibody reveals ebolavirus fusion loop as a site of vulnerability. Cell *169*, 891–904.e15.

STAR★METHODS

KEY RESOURCES TABLE

REAGENT or RESOURCE	SOURCE	IDENTIFIER
Antibodies		
ADI-15946	(Bornholdt et al., 2016); Adimab, LLC	GenBank: VH:KU602499 and VL:KU602500; RRID: AB_2750595
ADI-23774	this study; Adimab, LLC	RRID: AB_2750596
ADI-15878	(Bornholdt et al., 2016); Adimab, LLC	GenBank: VH:KU602365 and VL:KU602366; RRID: AB_2750594
CA45	(Zhao et al., 2017); M.J. Aman	N/A
ZMapp	(Qiu et al., 2014); Mapp Bio	N/A
MBP134^{AF}	this study; Mapp Bio	RRID: AB_2750598
MBP134	this study; Mapp Bio	RRID: AB_2750597
Mouse anti-human CD107a (clone H4A3)	BD Biosciences	RRID: AB_396136
Mouse anti-human CD3 (clone UCHT1)	BD Biosciences	RRID: AB_396952
Mouse anti-human CD56 (clone B159)	BD Biosciences	RRID: AB_396853
Mouse anti-human CD16 (clone 3G8)	BD Biosciences	RRID: AB_396864
Mouse anti-human IFNγ(clone B27)	BD Biosciences	RRID: AB_398580
Mouse anti-human MIP-1β (clone D21-1351)	BD Biosciences	RRID: AB_393549
Bacteria and Viruses		
rVSV-EBOV/Mayinga GP (EBOV/H.sap-tc/COD/76/Yambuku-Mayinga)	(Wong et al., 2010)	N/A
rVSV-SUDV/Boneface GP (SUDV/C.por-lab/ SSD/76/Boneface)	(Wec et al., 2016)	N/A
rVSV-BDBV GP (BDBV/H.sap/UGA/07/But-811250)	(Wec et al., 2016)	N/A
rVSV-TAFV ΔMuc GP (TAFV/H.sap-tc/CIV/94/CDC807212)	(Wec et al., 2016)	N/A
rVSV-BOMV GP/ (BOMV/M.con/SLE/16/MF319185)	(Goldstein et al., 2018)	N/A
rVSV-RESTV GP (RESTV/M.fas-tc/USA/89/Phi89-AZ-1435)	(Wec et al., 2016)	N/A
Mouse-adapted EBOV/Mayinga (EBOV-MA) (EBOV/M.mus-tc/COD/76/Yambuku-Mayinga)	(Bray et al., 1998); USAMRIID	N/A
Guinea pig-adapted EBOV/Mayinga (EBOV-GPA) (Ebola virus VECTOR/C.porcellus-lab/COD/76/Mayinga-GPA)	(Connolly et al., 1999);PHAC	N/A
Guinea pig-adapted SUDV/Boneface (SUDV-GPA) (Sudan virus/NML/C.porcellus-lab/SSD/76/Nzara-Boneface-GP)	(Wong et al., 2015); PHAC	N/A
EBOV/"Zaire1995" (EBOV/H.sap-tc/COD/95/Kik-9510621)	(Jahrling et al., 1999); USAMRIID	N/A
SUDV/Boneface (Sudan virus/H. sap-gp-tc/SDN/1976/Boneface-USAMRIID111808)	(Brannan et al., 2015); USAMRIID	N/A
BDBV (Bundibugyo virus/H. sap-tc/UGA/2007/Bundibugyo-200706291)	(Towner et al., 2008); USAMRIID	N/A
Chemicals, Peptides, and Recombinant Proteins		
Soluble GP EBOVΔMucΔTM	this study; Mapp Bio	N/A
Soluble GP SUDVΔMucΔTM	this study; Mapp Bio	N/A
Soluble GP BDBVΔMucΔTM	this study; Mapp Bio	N/A
Ultra-TMB colorimetric substrate	Thermo Fisher	Cat# 34029
Brefeldin A	Sigma Aldrich	Cat# B7651
GolgiStop	BD Biosciences	Cat# 554724
Freestyle 293 expression medium	Thermo Fisher	Cat# 12338002

(*Continued on next page*)

Continued

REAGENT or RESOURCE	SOURCE	IDENTIFIER
Critical Commercial Assays		
RosetteSep NK cell enrichment kit	Stem Cell Technologies	Cat# 15025
Experimental Models: Cell Lines		
HEK293T	ATCC	CRL-3216
293-Freestyle	Thermo Fisher	R79007
Vero	ATCC	CCL-81
Vero C1008 cells (VERO 76, clone E6, Vero E6)	ATCC	CRL-1586
Drosophila S2	Thermo Fisher	*R69007*
Primary human immune cells (NK cells)	MGH Blood Bank; Ragon Institute Clinical Core	N/A
Experimental Models: Organisms/Strains		
ΔXTFT N. *benthamiana*	(Olinger et al., 2012)	N/A
Mouse: Female BALB/cAnNCrl	Charles River	Strain code: 028
Mouse: B6.129S2-Ifnar1tm1Agt/Mmjax (Type 1 IFNα/βR−/−)	Jackson Labs	MMRRC: 32045-JAX
Hartley guinea pigs	Charles River	N/A
Software and Algorithms		
Prism	Graph Pad	https://www.graphpad.com/scientific-software/prism/
Other		
CellInsight CX5 High Content Screening (HCS) Platform	Thermo Fisher	CX51110
Biacore 8K	GE Healthcare	http://www.gelifesciences.com/en/be/shop/protein-analysis/spr-label-free-analysis/systems/biacore-8k-p-05540
Octet RED96 System	ForteBio, Pall LLC	https://www.fortebio.com/octet-RED96.html
Anti-human Fc (AHC) capture sensors	ForteBio, Pall LLC	18-5060
BD LSR2 flow cytometer	BD Biosciences	N/A

CONTACT FOR REAGENT AND RESOURCE SHARING

Further information and requests for resources and reagents should be directed to and will be fulfilled by Lead Contact, Dr. Kartik Chandran (kartik.chandran@einstein.yu.edu).

EXPERIMENTAL MODEL AND SUBJECT DETAILS

Cell Lines

Vero female African grivet monkey kidney cells and HEK293T female human embryonic kidney fibroblast cells obtained from American Type Culture Collection (ATCC) and maintained in high-glucose Dulbecco's modified Eagle medium (DMEM; Thermo Fisher, Carlsbad, CA) supplemented with 10% fetal bovine serum (Atlanta Biologicals, Flowery Branch, GA), 1% GlutaMAX (Thermo Fisher), and 1% penicillin-streptomycin (Thermo Fisher). Cells were maintained in a humidified 37°C, 5% CO2 incubator. Suspension adapted HEK293F (Thermo Fisher) were maintained in serum free Freestyle HEK293F expression medium (Thermo Fisher). Cells were maintained in a humidified 37°C, 8% CO2, 125 rpm shaking incubator. *Drosophila melanogaster* S2 cells (Thermo Fisher) were cultured in complete Schneider's medium at 27°C. Cell lines were not authenticated following purchase.

Culture of Primary Human Innate Immune Cells

Primary human NK cells from deidentified donors were cultured and maintained in RPMI1640 supplemented with 10% fetal bovine serum, L-Glutamine, and penicillin/streptomycin at 37°C in a humidified incubator at 5% CO2 for the duration of the assays.

Ethics Statement for Primary Human Innate Immune Cells

Innate immune effector cells were isolated from fresh peripheral blood samples collected by the Ragon Institute or the MGH Blood bank from healthy human volunteers. All subjects signed informed consent and the study was approved by the MGH Institutional

Review Board. Samples were collected from human adults older than 18 years of age, and were completely deidentified prior to use and thus, researchers were blinded to gender and age of donors.

Mice

Female BALB/c mice (Jackson Labs, Bar Harbor, ME), aged 10-12 weeks old and female Type 1 IFN α/β receptor knockout mice (Type 1 IFNα/β R$-/-$) (Jackson Labs) aged 6-8 weeks old were used for *in* vivo protection studies. Animals were provided food and water *ad libitum* and housed in individual ventilated cages.

Guinea Pigs

Female outbred Hartley guinea pigs (250-300 g), aged 4-6 weeks old, were purchased from Charles River Laboratories (Wilmington, MA). Animals were provided food and water *ad libitum* and given environmental enrichment according to the guidelines for the species. Cleaning of the animals was completed three times per week which included a complete cage and bedding material change. Animals were kept 2–3 per cage in the large shoe box cages from IVC Alternative Design. Each unit is ventilated with a HEPA blower system.

Animal Welfare Statement

Murine challenge studies were conducted under IACUC-approved protocols in compliance with the Animal Welfare Act, PHS Policy, and other applicable federal statutes and regulations relating to animals and experiments involving animals. The facility where these studies was conducted (USAMRIID) is accredited by the Association for Assessment and Accreditation of Laboratory Animal Care, International (AAALAC), and adheres to principles stated in the Guide for the Care and Use of Laboratory Animals, National Research Council, 2011. Guinea pig challenge studies were approved by the Animal Care Committee (ACC) of the Canadian Science Centre for Human and Animal Health (CSCHAH) in Winnipeg, Canada, in accordance with guidelines from the Canadian Council on Animal Care (CCAC).

Recombinant Vesicular Stomatitis Viruses (rVSVs)

Recombinant vesicular stomatitis Indiana viruses (rVSVs) expressing eGFP in the first position, and encoding representative GP proteins from EBOV/Mayinga (EBOV/H.sap-tc/COD/76/Yambuku-Mayinga), BDBV (BDBV/H.sap/UGA/07/But-811250), SUDV/Boneface (SUDV/C.por-lab/SSD/76/Boneface), BOMV (BOMV/M.con/SLE/16/MF319185), TAFV ΔMuc (TAFV/H.sap-tc/CIV/94/CDC807212), RESTV (RESTV/M.fas-tc/USA/89/Phi89-AZ-1435) in place of VSV G have been generated using a plasmid based rescue system in HEK293T and described previously (Goldstein et al., 2018; Ng et al., 2014; Wec et al., 2016; Whelan et al., 1995; Wong et al., 2010).

Authentic Filoviruses

The authentic filoviruses EBOV/"Zaire 1995" (EBOV/H.sap-tc/COD/95/Kik-9510621) (Jahrling et al., 1999), mouse-adapted EBOV/Mayinga (EBOV-MA) (Bray et al., 1998), SUDV/Boneface-USAMRIID111808, and BDBV/200706291 (Towner et al., 2008), Guinea pig-adapted EBOV/Mayinga (EBOV-GPA) (Ebola virus VECTOR/C.porcellus-lab/COD/76/Mayinga-GPA) (Connolly et al., 1999), Guinea pig-adapted SUDV/Boneface (SUDV-GPA) (Sudan virus/NML/C.porcellus-lab/SSD/76/Nzara-Boneface-GP) (Wong et al., 2015) were used in this study.

METHOD DETAILS

Expression and Purification of mAbs

Recombinant mAbs ADI-15946, ADI-23774 and ADI-15878 were produced in HEK293F cells (Thermo Fisher) by transient transfection, and purified by protein A affinity chromatography, as described previously (Wec et al., 2016). MBP134^{AF} (afucosylated) component mAbs were produced in ΔXTFT *N. benthamiana* tobacco plants via transient expression and purification as previously described (Olinger et al., 2012).

Expression and Purification of Recombinant GP Ectodomains

Ebolavirus GPs lacking the mucin domain and transmembrane domain (EBOV: aa32-632, Δ311-463), (SUDV: aa1-637, Δ270-473), (BDBV: aa1-640, Δ312-470) were produced from stable *Drosophila melanogaster* S2 cell lines. Briefly, Effectene (QIAGEN) was used to transfect S2 cells with a modified pMT-puro vector plasmid containing the GP gene of interest, followed by stable selection in the presence of puromycin (6 μg/mL). Cells were cultured at 27°C in complete Schneider's medium and then adapted to HyClone SFM4insect media (GE Healthcare) for large-scale expression in 2-L Erlenmeyer flasks. Expression was induced with 1 mM $CuSO_4$, and supernatant harvested when cell viability dropped below 80%, as determined by a trypan blue exclusion assay. All GPs were engineered with a C-terminal double Strep-tag to facilitate purification using a StrepTrap HP 5 mL prepacked column (GE Healthcare) using an AKTA pure 25M3 (GE Healthcare) and then further purified over a Superdex Increase 200 in PBS.

VSV Infectivity Measurements and Neutralization Assays

Viral infectivity was determined by automated counting of eGFP+ cells (infectious units; IU) using a CellInsight CX5 imager (Thermo Fisher) at 12–14 h post-infection. For mAb neutralization experiments, pre-titrated amounts of recombinant vesicular stomatitis viruses (rVSVs) expressing eGFP and GP from EBOV, BDBV, TAFV, SUDV, RESTV and BOMV particles (MOI ≈1 IU per cell) were incubated with increasing concentrations of test mAb at room temp for 1 h, and then added to confluent Vero cell monolayers in 96-well plates (Goldstein et al., 2018; Wec et al., 2016; Wong et al., 2010). Viral neutralization data were subjected to nonlinear regression analysis to derive IC_{50} values (4-parameter, variable slope sigmoidal dose-response equation; GraphPad Prism, La Jolla, CA).

Authentic Filovirus Microneutralization Assays

The authentic filoviruses EBOV/"Zaire 1995" (EBOV/H.sap-tc/COD/95/Kik-9510621) (Jahrling et al., 1999), SUDV/Boneface-USAM-RIID111808 (Brannan et al., 2015), and BDBV/200706291 (Towner et al., 2008) were used in this study. Antibodies were diluted to indicated concentrations in culture media and incubated with virus for 1 h. Vero E6 cells were exposed to antibody/virus inoculum at an MOI of 0.2 (EBOV, BDBV) or 0.5 (SUDV) plaque-forming unit (PFU) per cell for 1 h. Antibody/virus inoculum was then removed, and fresh culture media was added. At 48 h post-infection, cells were fixed, and infected cells were immunostained and quantitated by automated fluorescence microscopy, as described (Wec et al., 2016).

ADI-15946 Affinity Maturation

Affinity maturation libraries were generated by introducing diversity into the ADI-15946 heavy and light chains via site-saturation mutagenesis. Degenerate oligonucleotides sampling all 20 amino acids at each position within each CDR were incorporated into ADI-15946 via DNA shuffling, as described previously (Stemmer, 1994). The resulting libraries were then transformed into *Saccharomyces cerevisiae* using homologous recombination, as described (Xu et al., 2013). To identify improved variants, selections were carried out using flow cytometry as generally described (Chao et al., 2006). Briefly, libraries were incubated with titrating amounts of a recombinant SUDV monomer and sorted by FACS. Variants with improved binding affinities were identified from the HC and LC libraries by the second and third rounds of selection, respectively (see Figure S1). Selection outputs were plated, and colonies were picked for sequence analysis and IgG production. Beneficial mutations identified from the HC and LC library selections were then rationally combined and the resulting variants were screened for further improvements in binding activity via biolayer interferometry assays (ForteBio, Pall LLC).

GP:mAb Binding ELISA

To compare binding of ADI-15946 and ADI-23774 to SUDV, EBOV, and BDBV GP displayed on rVSVs (see Figure S2), normalized amounts of sucrose gradient purified rVSVs bearing SUDV, EBOV, and BDBV GPs were coated overnight onto plates at 4°C. Plates were then blocked with PBS containing 3% bovine serum albumin (PBSA) and incubated with dilutions of test antibody. Bound Abs were detected with anti-human IgG conjugated to horseradish peroxidase (Santa Cruz Biotechnology, Dallas, TX) and Ultra-TMB colorimetric substrate (Thermo Fisher). All incubations were performed for 1 h at 37°C.

GP:mAb Kinetic Binding Analysis by Biolayer Interferometry (BLI)

The OctetRed system (ForteBio) was used to measure binding competition to a trimeric EBOV GP ectodomain between ADI-15946, ADI-15878 and CA45. Ni-NTA (NTA, ForteBio) sensors were used to capture hexahistidine-tagged EBOV GP trimers (40 μg/mL) in 1 × Kinetics Buffer (PBS supplemented with 0.002% Tween-20 and 1 mg/mL BSA). Binding of test mAbs to GP was performed in two separate association stages. The sensors were dipped in the first test mAb at 50 μg/mL and then transferred to the next test mAb solution at 50 μg/mL also containing 25 μg/mL of the first test mAb. The baseline and dissociation steps were carried out in 1 × Kinetics Buffer according to the manufacturer's recommendations.

GP:mAb Kinetic Binding Analysis by Surface Plasmon Resonance (SPR)

SPR biosensor analysis was conducted at 25°C in a HBS-EP+ buffer system (10 mM HEPES [pH 7.4], 150 mM NaCl, 3 mM EDTA, 0.05% Surfactant P20) with 0.1% BSA using a Biacore 8K optical biosensor (GE Healthcare, Marlboro, MA) docked with a C1 sensor chip (GE Healthcare). The sample compartment was maintained at 10°C. Goat anti-human IgG capture antibody (Jackson ImmunoResearch, West Grove, PA) was immobilized (990 ± 23 RU) to both flow cells of the sensor chip using standard amine coupling chemistry. This surface provided a format for reproducible capture of fresh analysis antibody after each regeneration step. Flow cell 2 was used to analyze captured antibody (137 ± 8 RU) while flow cell 1 was used as a reference flow cell. Antigen concentrations ranging from 81 to 0.3 nM (3-fold dilutions) were prepared in running buffer. Each of the antigen concentrations were run as a single replicate. Three blank (buffer) injections were run and used to assess and subtract system artifacts. The association (420 s) and dissociation (1800 s) phases for all antigen concentrations were monitored at a flow rate of 25 μL per min. The surface was regenerated with two injections of 10 mM glycine[pH 1.5] for 30 s, at a flow rate of 30 μL per min. The data were aligned, double referenced, and fit using the 1:1 binding model from the Biacore 8K Evaluation Software, version 1.0. Sensorgram images were generated in GraphPad Prism.

Antibody-Mediated Activation of Human NK (Natural Killer) Cells

To evaluate the ability of *N. benthamiana*- and HEK293-produced mAbs (afucosylated and fucosylated, respectively) to activate NK function, human NK cells were enriched from the peripheral blood of four different human donors by negative selection using the RosetteSep kit (STEMCELL Technologies, Cambridge, MA) followed by Ficoll separation. NK cells were rested overnight in the presence of 1 ng/mL recombinant IL-15 (PeproTech, Rocky Hill, NJ). 3 ng per well of EBOV GP was coated on a Nunc Maxisorp ELISA plate (Thermo Fisher) at 4°C overnight, and plates were blocked with 5% BSA prior to addition of dilutions of antibodies (10 μg/mL) in PBS for 2 hours at 37°C. Unbound antibodies were removed by washing wells 3 × with PBS prior to addition of NK cells. The NK cells were added at 5×10^4 cells/well in the presence of brefeldin A (Sigma Aldrich), GolgiStop (BD Biosciences, Franklin Lake, NJ), and α–CD107a-PE-Cy5 antibody, and incubated for 5 h at 37°C. NK cells were stained with flow cytometry antibodies for the following surface markers: α–CD3-AlexaFluor700, α–CD56-PE-Cy7, and α–CD16-APC-Cy7, followed by intracellular staining for IFNα (FITC) and MIP-1β (PE). All antibody conjugates were from BD Biosciences. Cells were analyzed by flow cytometry on a BD LSR2 flow cytometer and data was processed using FlowJo software (Ashland, OR).

EBOV and SUDV Challenge Studies in Mice

10–12-week old female BALB/c mice (Jackson Labs, Bar Harbor, ME) were challenged via the intraperitoneal (i.p.) route with mouse-adapted EBOV/Mayinga (EBOV-MA) (Bray et al., 1998) (100 PFU; ~3,000 LD_{50}). Mice were treated i.p. 3 days post-challenge with PBS vehicle or 300 μg of each mAb (0.3 mL volume, ≈15 mg mAb/kg). Animals were observed daily for clinical signs of disease and lethality for 28 days. Daily observations were increased to a minimum of twice daily while mice were exhibiting signs of disease. Moribund mice were humanely euthanized on the basis of IACUC-approved criteria. 6–8-week old female Type 1 IFN α/β receptor knockout mice (Type 1 IFNα/β R−/−) (Jackson Labs) were challenged with WT SUDV (1000 PFU i.p.). Animals were treated i.p. 1 and 4 days post-challenge with PBS vehicle or 300 μg (0.3 mL volume, ≈15 mg mAb/kg) per dose and monitored and euthanized as above.

EBOV and SUDV Challenge Studies in Guinea Pigs

4-6-week old female guinea pigs (250-300 g) were randomly assigned to experimental groups with 6 guinea pigs per group (n = 6). All animals were challenged via the i.p. route with a 1000 LD_{50} of EBOV-GPA (Connolly et al., 1999) or SUDV-GPA (Wong et al., 2015) in 1 mL of DMEM. ADI-15878, ZMapp, MBP134, and $MBP134^{AF}$ were administered i.p. at 3 days post-challenge (EBOV-GPA), or 4 or 5 days post-challenge (SUDV-GPA). Control-group animals received DPBS. Animals were observed for clinical signs of disease, survival and weight change for up to 20 days, and survival was monitored for an additional 12 days.

QUANTIFICATION AND STATISTICAL ANALYSIS

Statistical Analysis

Dose-response neutralization curves were fit to a logistic equation by nonlinear regression analysis. 95% confidence intervals (95% CI) for the extracted IC_{50} parameter were estimated under the assumption of normality. Analysis of survival curves was performed with the Mantel-Cox (log-rank) test. Statistical comparisons of NK cell activity were carried out by one-way ANOVA with Tukey's correction for multiple comparisons testing. Testing level (alpha) was 0.05 for all statistical tests. Detailed statistical comparisons on groups in Figures 6 and 7 are shown in Figure S3. Technical and biological replicates are indicated in the Figure Legends. All analyses were carried out in GraphPad Prism.

Cell Host & Microbe, Volume *25*

Supplemental Information

Development of a Human Antibody Cocktail that Deploys Multiple Functions to Confer Pan-Ebolavirus Protection

Anna Z. Wec, Zachary A. Bornholdt, Shihua He, Andrew S. Herbert, Eileen Goodwin, Ariel S. Wirchnianski, Bronwyn M. Gunn, Zirui Zhang, Wenjun Zhu, Guodong Liu, Dafna M. Abelson, Crystal L. Moyer, Rohit K. Jangra, Rebekah M. James, Russell R. Bakken, Natasha Bohorova, Ognian Bohorov, Do H. Kim, Michael H. Pauly, Jesus Velasco, Robert H. Bortz III, Kevin J. Whaley, Tracey Goldstein, Simon J. Anthony, Galit Alter, Laura M. Walker, John M. Dye, Larry Zeitlin, Xiangguo Qiu, and Kartik Chandran

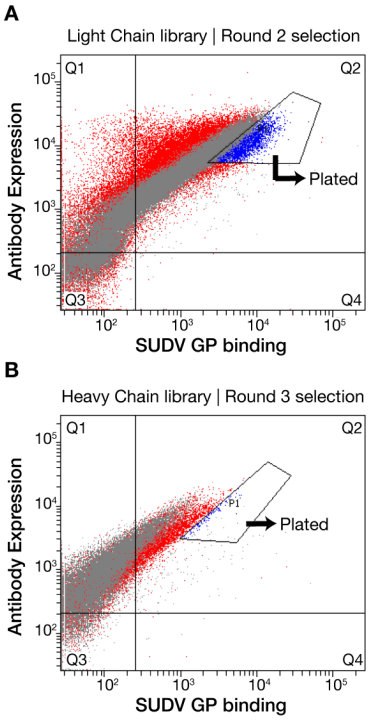

Figure S1. Specificity maturation of ADI-15946, related to Figure 2

(A–B) ADI-15946 variant libraries incorporating mutations in each CDR in the antibody light chain (LC) (A) or heavy chain (HC) (B) were expressed by yeast surface display. Variants with improved binding to a purified SUDV GP ectodomain were identified and isolated by fluorescence-activated cell sorting after the second (LC) and third (HC) rounds of selection (events colored blue above). Selected cells were plated, and colonies were picked for sequence analysis and IgG production. Beneficial LC and HC mutations were then rationally combined, and the resulting variants were screened for further improvements in binding activity (See STAR Methods for details).

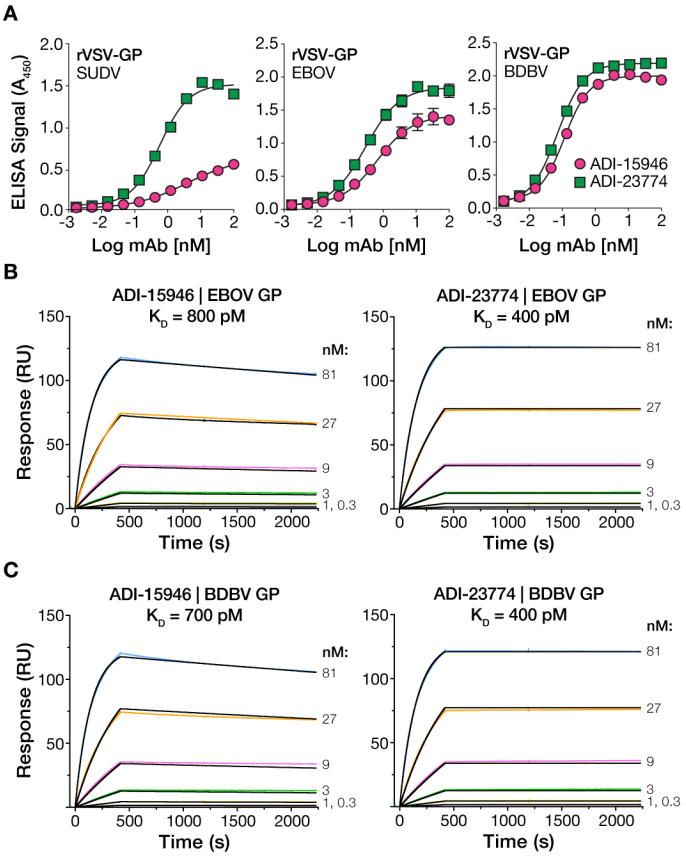

D

Antibody	k_{on} ($M^{-1}s^{-1}$)	k_{off} (s^{-1})	K_D (M)
SUDV GP			
ADI-15946	2.6×10^{5}	3.2×10^{-4}	1.2×10^{-9}
ADI-23774	2.3×10^{5}	3.8×10^{-5}	1.6×10^{-10}
EBOV GP			
ADI-15946	8.1×10^{4}	6.1×10^{-5}	7.5×10^{-10}
ADI-23774	7.5×10^{4}	2.9×10^{-5}	3.8×10^{-10}
BDBV GP			
ADI-15946	8.5×10^{4}	6.1×10^{-5}	7.1×10^{-10}
ADI-23774	8.0×10^{4}	2.9×10^{-5}	3.6×10^{-10}

Figure S2. Binding properties of ADI-23774, related to Figure 2

(A) Capacity of ADI-15946 and ADI-23774 to recognize rVSVs bearing SUDV, EBOV, and BDBV GP in an ELISA. Averages±SD (n=3) from two independent experiments. (B–C) Sensorgrams for IgG interactions with EBOV (B) and BDBV GP (C) with ADI-15946 (left) and ADI-23774 (right). Experimental curves (colored traces) were fit using a 1:1 binding model (black traces). The corresponding flow analyte (GP) concentration is indicated at the right of each curve. (D) Kinetic binding constants for each GP:IgG interaction derived from the binding models in panels B–C and in Figure 2A–B. Results from a representative

experiment are shown. k_{on}, association rate constant. k_{off}, dissociation rate constant. K_D, equilibrium dissociation constant.

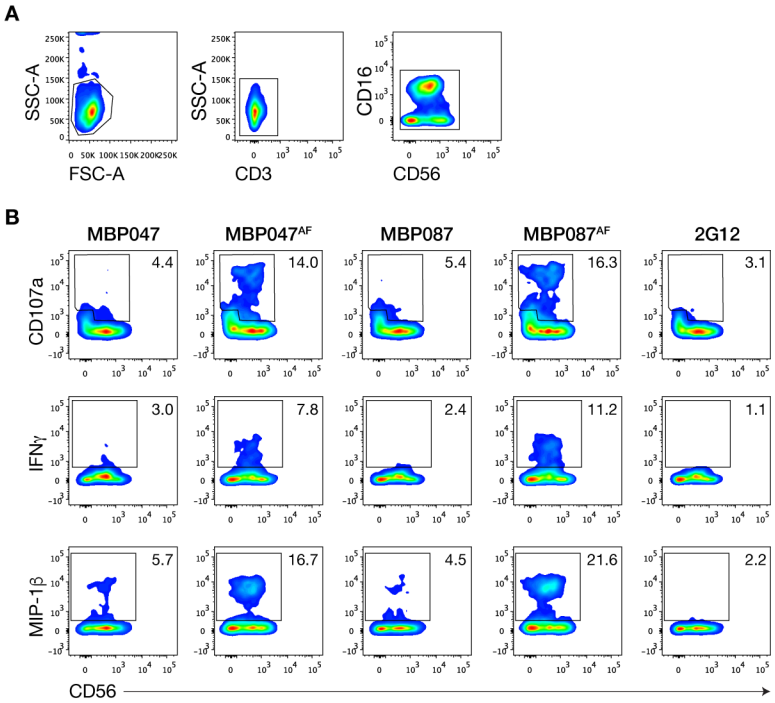

Figure S3. Flow-cytometric gating strategy for antibody-dependent NK cell activation assay, related to Figure 7

(A) Gating strategy used to enrich cytotoxic NK cells ($CD3^{-}/CD56^{dim}/CD16^{+}$) from the peripheral blood of human donors. Cells were gated first on forward scatter and side scatter, followed by gating on $CD3^{-}$ cells. CD16 and CD56 expression were confirmed on $CD3^{-}$ cells, and because CD16 is downregulated upon activation, both $CD16^{-}$ and CD16 cells were analyzed for activation. (B) Flow-cytometric analysis of indicated antibodies for markers of NK cell degranulation (CD107a; top row), production of IFN-γ (middle row), and MIP-1β (bottom row). Positive gates and the percentage of parent gate (CD16/CD56) are indicated. Representative flow cytometry plots are shown.

Groups compared[a]	Challenge virus	dpi[b]	χ^2	df[c]	*P* value	Summary
DPBS vs. MBP134 (0.5 mg)	EBOV-GPA	3	4.698	1	0.0302	*
DPBS vs. MBP134 (1.3 mg)	EBOV-GPA	3	9.135	1	0.0025	**
DPBS vs. MBP134 (2.5 mg)	EBOV-GPA	3	9.135	1	0.0025	**
DPBS vs. MBP134 (3.3 mg)	EBOV-GPA	3	9.135	1	0.0025	**
MBP134 (1.3 mg) vs. MBP134 (2.5 mg)	EBOV-GPA	3	6.457	1	0.0110	*
MBP134 (1.3 mg) vs. MBP134 (3.3 mg)	EBOV-GPA	3	7.942	1	0.0048	**
ADI-15878 (2.5 mg) vs. MBP134 (2.5 mg)	EBOV-GPA	3	0.987	1	0.3206	ns
ADI-15878 (5 mg) vs. MBP134 (3.3 mg)	EBOV-GPA	3	3.669	1	0.0554	ns

Table S1. Statistical comparison of survival curves between groups in the guinea pig challenge studies with MBP134, related to Figure 6

[a]Survival curves obtained with the indicated groups were compared by the Mantel-Cox (log-rank) test.

[b]dpi, day post-infection on which cocktail was administered

[c]df, degrees of freedom (number of groups - 1)

Groups compared[a]	Challenge virus	dpi[b]	χ^2	df[c]	*P* value	Summary
DPBS vs. MBP134^{AF} (0.5 mg)	EBOV-GPA	3	4.698	1	0.0302	*
DPBS vs. MBP134^{AF} (1.3 mg)	EBOV-GPA	3	9.135	1	0.0025	**
DPBS vs. MBP134^{AF} (2.5 mg)	EBOV-GPA	3	9.135	1	0.0025	**
DPBS vs. MBP134^{AF} (3.3 mg)	EBOV-GPA	3	9.135	1	0.0025	**
MBP134^{AF} (0.5 mg) vs. MBP134^{AF} (1.3 mg)	EBOV-GPA	3	8.143	1	0.0043	**
MBP134^{AF} (0.5 mg) vs. MBP134^{AF} (2.5 mg)	EBOV-GPA	3	5.577	1	0.0182	*
MBP134^{AF} (1.3 mg) vs. MBP134 (1.3 mg)	EBOV-GPA	3	7.942	1	0.0048	**
DPBS vs. MBP134^{AF} (0.3 mg)	SUDV-GPA	4	4.771	1	0.0289	*
DPBS vs. MBP134^{AF} (0.5 mg)	SUDV-GPA	4	10.56	1	0.0012	**
DPBS vs. MBP134^{AF} (0.8 mg)	SUDV-GPA	4	10.56	1	0.0012	**
DPBS vs. MBP134^{AF} (1.3 mg)	SUDV-GPA	4	10.56	1	0.0012	**
DPBS vs. MBP134^{AF} (2.5 mg)	SUDV-GPA	4	10.56	1	0.0012	**
DPBS vs. MBP134^{AF} (1.3 mg)	SUDV-GPA	4	7.942	1	0.0048	**
MBP134^{AF} (0.3 mg) vs. MBP134^{AF} (1.3 mg)	SUDV-GPA	4	6.435	1	0.0112	*
MBP134^{AF} (0.3 mg) vs. MBP134^{AF} (2.5 mg)	SUDV-GPA	4	8.008	1	0.0047	**
DPBS vs. MBP134^{AF} (2.5 mg)	SUDV-GPA	5	6.667	1	0.0098	**
DPBS vs. MBP134^{AF} (5.0 mg)	SUDV-GPA	5	10.56	1	0.0012	**
MBP134^{AF} (2.5 mg) vs. MBP134^{AF} (5.0 mg)	SUDV-GPA	5	2.195	1	0.1385	ns

Table S2. Statistical comparison of survival curves between groups in the guinea pig challenge studies with MBP134^{AF}, related to Figure 7

[a]Survival curves obtained with the indicated groups were compared by the Mantel-Cox (log-rank) test.

[b]dpi, day post-infection on which cocktail was administered

[c]df, degrees of freedom (number of groups - 1)